

# Projector formalism for kept and discarded spaces of matrix product states

Andreas Gleis,<sup>1</sup> Jheng-Wei Li,<sup>1</sup> and Jan von Delft<sup>1</sup>

<sup>1</sup>*Arnold Sommerfeld Center for Theoretical Physics, Center for NanoScience, and Munich Center for Quantum Science and Technology, Ludwig-Maximilians-Universität München, 80333 Munich, Germany*

(Dated: June 1, 2023)

Any matrix product state  $|\Psi\rangle$  has a set of associated kept and discarded spaces, needed for the description of  $|\Psi\rangle$ , and changes thereof, respectively. These induce a partition of the full Hilbert space of the system into mutually orthogonal spaces of irreducible  $n$ -site variations of  $|\Psi\rangle$ . Here, we introduce a convenient projector formalism and diagrammatic notation to characterize these  $n$ -site spaces explicitly. This greatly facilitates the formulation of MPS algorithms that explicitly or implicitly employ discarded spaces. As an illustration, we derive an explicit expression for the  $n$ -site energy variance and evaluate it numerically for a model with long-range hopping. We also describe an efficient algorithm for computing low-lying  $n$ -site excitations above a finite MPS ground state.

DOI:

## I. INTRODUCTION

Matrix product states (MPS) are widely used for the numerical description of quantum systems defined on one- or two-dimensional lattices. Well-known MPS-based algorithms include ground state searches and time evolution using the density matrix renormalization group (DMRG and tDMRG) [1–6], time-evolving block decimation (TEBD) methods [7–9], or the time-dependent variational principle (TDVP) [10–14]; and the computation of spectral information using the numerical renormalization group (NRG) [15–17], DMRG [18–21], or so-called post-MPS approaches [14, 22]; see Refs. [23–25] for reviews.

All such algorithms involve update steps: a quantum state of interest,  $|\Psi\rangle$ , is represented in MPS form, and its constituent tensors are updated, e.g. during optimization or time evolution. During an update, highly relevant information is *kept* ( $\kappa$ ) and less relevant information *discarded* ( $\mathsf{D}$ ). A sequence of updates thereby endows the full Hilbert space of the system,  $\mathbb{V}$ , with a structure of intricately nested  $\kappa$  or  $\mathsf{D}$  subspaces, changing with each update, containing states from  $\mathbb{V}$  which either do ( $\kappa$ ) or do not ( $\mathsf{D}$ ) contribute to the description of  $|\Psi\rangle$ .

The nested structure of  $\mathbb{V}$  is rarely made explicit in the formulation of MPS algorithms. A notable exception is NRG, where  $\mathsf{D}$  states are used to construct a complete basis [26] of approximate energy eigenstates for  $\mathbb{V}$ , facilitating the computation of time evolution or spectral information [16, 17]. For the computation of local multipoint correlators [27] using NRG, it has proven useful to elucidate the structure of  $\kappa$  and  $\mathsf{D}$  subspaces by introducing projectors having these subspaces as their images. The orthogonality properties of  $\kappa$  and  $\mathsf{D}$  projectors bring structure and clarity to the description of rather complex algorithmic strategies.

Inspired by the convenience of  $\kappa$  and  $\mathsf{D}$  projectors in the context of NRG, we here introduce an analogous but more general  $\kappa, \mathsf{D}$  projector formalism and diagrammatic conventions suitable for the description of arbitrary MPS algorithms. In particular, our  $\kappa, \mathsf{D}$  projectors offer a

natural language for the formulation of algorithms that explicitly or implicitly employ discarded spaces; this includes algorithms evoking the notion of tangent spaces [10, 12–14, 22] and generalizations thereof, as will be described later.

To formulate the goals of this paper, we here briefly indicate how the nested subspaces mentioned above come about. Concrete constructions follow in later sections.

An MPS  $|\Psi\rangle$  written in canonical form is defined by a set of isometric tensors [23]. The image space of an isometric tensor, its *kept* space, is needed for the description of  $|\Psi\rangle$ . The orthogonal complement of the kept space, its *discarded* space, is not needed for  $|\Psi\rangle$  itself, but for the description of changes of  $|\Psi\rangle$  due to an update step, e.g. during variational optimization, time evolution, or the computation of excitations above the ground state. Any such change can be assigned to one of the subspaces  $\mathbb{V}^{ns}$  in the nested hierarchy

$$\mathbb{V}^{0s} \subset \mathbb{V}^{1s} \subset \mathbb{V}^{2s} \subset \dots \subset \mathbb{V}^{\mathcal{L}s} = \mathbb{V}, \quad (1)$$

where  $\mathbb{V}$  is the full Hilbert space of a system of  $\mathcal{L}$  sites,  $\mathbb{V}^{ns}$  the subspace spanned by all  $n$ -site ( $ns$ ) variations of  $|\Psi\rangle$ , and  $\mathbb{V}^{0s} = \text{span}\{|\Psi\rangle\}$  the one-dimensional space spanned by the reference MPS itself. The orthogonality of kept and discarded spaces induces a partition of each  $\mathbb{V}^{ns}$  into nested orthogonal subspaces [6, 28], such that

$$\mathbb{V}^{ns} = \oplus_{n'=0}^n \mathbb{V}^{n'\perp}, \quad (2)$$

where  $\mathbb{V}^{n\perp}$  is the subspace of  $\mathbb{V}^{ns}$  spanned by all irreducible  $ns$  variations not expressible through  $n'$ 's variations with  $n' < n$ , and  $\mathbb{V}^{0\perp} = \mathbb{V}^{0s}$ . In particular, the full Hilbert space can be represented as  $\mathbb{V} = \oplus_{n=0}^{\mathcal{L}} \mathbb{V}^{n\perp}$ .

The subspaces defined above underlie, implicitly or explicitly, all MPS algorithms.  $\mathbb{V}^{1s}$  is the so-called tangent space of  $|\Psi\rangle$ , i.e. the space of all one-site ( $1s$ ) variations of  $|\Psi\rangle$ . It plays an explicit role in numerous recent MPS algorithms, such as TDVP time-evolution, or the description of translationally invariant MPS and their excitations [13, 14, 28]. It also features implicitly in MPS algorithms

formulated using 1s update schemes, such as the 1s formulation of DMRG [23], because 1s updates explore states from  $\mathbb{V}^{1s}$ . Likewise, the space  $\mathbb{V}^{2s}$  implicitly underlies all 2s MPS algorithms such as 2s DMRG ground state search, 2s time-dependent DMRG (tDMRG), or 2s TDVP, in that 2s updates explore states from  $\mathbb{V}^{2s}$ . Moreover,  $\mathbb{V}^{1\perp}$  and  $\mathbb{V}^{2\perp}$  are invoked explicitly when computing the 2s energy variance, an error measure for MPS ground state searches introduced in Ref. [6]. Finally,  $\mathbb{V}^{ns}$  is implicitly invoked in MPS algorithms defining excited states of translationally invariant MPS through linear combinations of local excitations defined on  $n$  sites [22].

The construction of a basis for  $\mathbb{V}^{ns}$  and  $\mathbb{V}^{n\perp}$  is well known for  $n = 1$  [12], and for  $n = 2$  it is outlined in Ref. [6]. However, we are not aware of a general, explicit construction for  $n > 2$ , as needed, e.g., to compute the  $ns$  energy variance. Here, we explicitly construct projectors,  $\mathcal{P}^{ns}$  and  $\mathcal{P}^{n\perp}$ , having  $\mathbb{V}^{ns}$  and  $\mathbb{V}^{n\perp}$  as images, respectively. For  $n = 1$ , this amounts to a construction of a basis for the tangent space  $\mathbb{V}^{1s}$ . More generally, our  $\kappa, D$  projector formalism used to construct  $\mathcal{P}^{ns}$  and  $\mathcal{P}^{n\perp}$  greatly facilitates the formulation of MPS algorithms that explicitly or implicitly employ discarded spaces. As an illustration, we derive an explicit expression for the  $n$ -site energy variance, generalizing the error measure proposed in Ref. [6], and evaluate it numerically for a model with long-range hopping, the Haldane-Shastry model. We also show how the multiparticle  $ns$  excitations proposed in Ref. [22] are formulated in our scheme, and propose a strategy for computing them explicitly, for any  $n$ .

We expect that the  $\kappa, D$  projector formalism developed here will be particularly useful for improving the efficiency of MPS algorithms by incorporating information from  $\mathbb{V}^{n\perp}$  into suitably expanded versions of  $\mathbb{V}^{(n' < n)s}$  without fully computing  $\mathbb{V}^{n\perp}$ . For example, we have recently developed a scheme, called controlled bond expansion, which incorporates 2s information into 1s updates for DMRG ground state search [29] and TDVP time evolution [30], in a manner requiring only 1s costs.

This paper is structured as follows. In Sec. II we collect some well-known facts about MPSs, and formally define the associated kept and discarded spaces and corresponding projectors. Section III, the heart of this paper, describes the construction of the  $\mathcal{P}^{ns}$  and  $\mathcal{P}^{n\perp}$  projectors for general  $n$ . As applications of our projector formalism, we compute the  $ns$  energy variance of the Haldane-Shastry model in Sec. IV, and describe the construction and computation of  $ns$  excitations in Sec. V. We end with a brief outlook in Sec. VI.

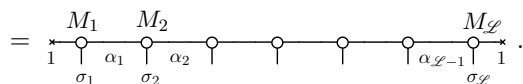
## II. MPS BASICS

This section offers a concise, tutorial-style summary of MPS notation and the associated diagrammatics. Moreover, we formalize the notion of kept spaces, needed to describe an MPS  $|\Psi\rangle$ , and discarded spaces, needed to describe changes to it at specified sites. We also recapit-

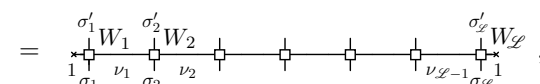
ulate the definition of local bond, 1s and 2s projectors routinely used in 1s and 2s MPS algorithms.

### A. Basic MPS notation

Consider a quantum chain with sites labeled  $\ell = 1, \dots, \mathcal{L}$ . Let each site be represented by a  $d$ -dimensional Hilbert space,  $\mathbb{V}_\ell$ , with local basis states  $|\sigma_\ell\rangle$ ,  $\sigma_\ell = 1, \dots, d$ . The full Hilbert space is  $\mathbb{V} = \prod_{\ell} \mathbb{V}_\ell = \text{span}\{|\sigma\rangle\}$ , with basis states  $|\sigma\rangle = |\sigma_1\rangle|\sigma_2\rangle\cdots|\sigma_{\mathcal{L}}\rangle$ . Any state  $|\Psi\rangle = |\sigma\rangle\Psi^\sigma \in \mathbb{V}$  can be written as an open boundary MPS, with wavefunction of the form

$$\Psi^\sigma = [M_1]_{1\alpha_1}^{\sigma_1} [M_2]_{\alpha_1\alpha_2}^{\sigma_2} \cdots [M_{\mathcal{L}}]_{\alpha_{\mathcal{L}-1}1}^{\sigma_{\mathcal{L}}} \quad (3)$$


(This diagram depicts both the wavefunction  $\Psi$  and the corresponding state  $|\Psi\rangle$ .) For clarity, we do not use ellipses in our MPS diagrams, but instead draw them for some small choice of  $\mathcal{L}$ , e.g.  $\mathcal{L} = 7$  above. Sums over repeated indices are implied throughout, and depicted diagrammatically by bonds. Each  $M_\ell$  is a three-leg tensor with elements  $[M_\ell]_{\alpha_{\ell-1}\alpha_\ell}^{\sigma_\ell}$ . Its physical and virtual bond indices,  $\sigma_\ell$  and  $\alpha_{\ell-1}, \alpha_\ell$ , have dimensions  $d$  and  $D_{\ell-1}, D_\ell$ , respectively. The outermost bonds, to dummy sites represented by crosses, have  $D_0 = D_{\mathcal{L}} = 1$ . The bond dimensions  $D_\ell$  are adjustable parameters, controlling the amount of entanglement an MPS can encode. (In the literature, it is common practice to drop the subscript on  $D_\ell$  for brevity, understanding that  $D$  can nevertheless vary from bond to bond.) Likewise, a Hamiltonian acting within  $\mathbb{V}$ ,  $\mathcal{H} = |\sigma\rangle H^{\sigma\sigma'} \langle\sigma'|$ , can be expressed as an MPO, with

$$H^{\sigma\sigma'} = [W_1]_{1\nu_1}^{\sigma_1\sigma'_1} [W_2]_{\nu_1\nu_2}^{\sigma_2\sigma'_2} \cdots [W_{\mathcal{L}}]_{\nu_{\mathcal{L}-1}1}^{\sigma_{\mathcal{L}}\sigma'_{\mathcal{L}}}, \quad (4)$$


where the four-leg tensors  $W_\ell$  have elements  $[W_\ell]_{\nu_{\ell-1}\nu_\ell}^{\sigma_\ell\sigma'_\ell}$ , and the virtual bond indices  $\nu_\ell$  have dimensions  $w_\ell$ .

Any MPS wavefunction can be brought into canonical form w.r.t. an “orthogonality center” at site  $\ell \in [1, \mathcal{L}]$ , or w.r.t. bond  $\ell$  connecting sites  $\ell$  and  $\ell + 1$ ,

$$\Psi^\sigma = \begin{array}{c} A_1 \quad A_{\ell-1} \quad C_\ell \quad B_{\ell+1} \quad B_{\mathcal{L}} \\ \text{---} \text{---} \text{---} \text{---} \text{---} \\ \sigma_1 \quad \sigma_{\ell-1} \quad \sigma_\ell \quad \sigma_{\ell+1} \quad \sigma_{\mathcal{L}} \end{array}, \quad (5)$$

where we indicated some of the bond dimensions. Here,  $A_{\tilde{\ell}}$  and  $B_{\tilde{\ell}}$  (with  $1 \leq \tilde{\ell} < \ell < \tilde{\ell}' \leq \mathcal{L}$ ) satisfy the relations

$$\begin{aligned} [A_{\tilde{\ell}}^\dagger]_{\alpha\bar{\alpha}}^\sigma [A_{\tilde{\ell}}]_{\bar{\alpha}\alpha'}^\sigma &= [\mathbb{1}_{\tilde{\ell}}^K]_{\alpha\alpha'}, & [B_{\tilde{\ell}'}]_{\alpha\bar{\alpha}}^\sigma [B_{\tilde{\ell}'}^\dagger]_{\bar{\alpha}\alpha'}^\sigma &= [\mathbb{1}_{\tilde{\ell}'}^K]_{\alpha\alpha'}, \\ \bar{\alpha} \bigcirc_{\alpha}^{\alpha'} &= \left( \alpha' = [\mathbb{1}_{\tilde{\ell}}^K]_{\alpha\alpha'}, \quad \alpha \bigcirc_{\alpha'}^{\alpha} = \alpha' \right) = [\mathbb{1}_{\tilde{\ell}-1}^K]_{\alpha\alpha'}, & (6) \end{aligned}$$

or  $A_{\tilde{\ell}}^\dagger A_{\tilde{\ell}} = \mathbb{1}_{\tilde{\ell}}^\kappa$ ,  $B_{\tilde{\ell}} B_{\tilde{\ell}'}^\dagger = \mathbb{1}_{\tilde{\ell}'-1}^\kappa$  for short, where  $\mathbb{1}_{\tilde{\ell}}^\kappa$  denotes a  $D_{\tilde{\ell}} \times D_{\tilde{\ell}}$  unit matrix. (The superscript  $\kappa$  stands for “kept”, for reasons explained below.) The open triangles representing  $A_{\tilde{\ell}}$  and  $B_{\tilde{\ell}}$  are oriented such that their diagonals face left or right, respectively. The orthogonality center can be shifted left or right by using singular value decomposition (SVD) to express it as  $C_{\tilde{\ell}} = U_{\tilde{\ell}-1} S_{\tilde{\ell}-1} B_{\tilde{\ell}}$  or  $C_{\tilde{\ell}} = A_{\tilde{\ell}} S_{\tilde{\ell}} V_{\tilde{\ell}}^\dagger$ :

$$\begin{array}{c} A_{\tilde{\ell}-1} \quad C_{\tilde{\ell}} \\ \text{---} \text{---} \end{array} = \begin{array}{c} A_{\tilde{\ell}-1} \quad U_{\tilde{\ell}-1} \quad S_{\tilde{\ell}-1} \quad B_{\tilde{\ell}} \\ \text{---} \text{---} \text{---} \end{array} = \begin{array}{c} C_{\tilde{\ell}-1} \quad B_{\tilde{\ell}} \\ \text{---} \text{---} \end{array}, \quad (7)$$

$$\begin{array}{c} C_{\tilde{\ell}} \quad B_{\tilde{\ell}+1} \\ \text{---} \text{---} \end{array} = \begin{array}{c} A_{\tilde{\ell}} \quad S_{\tilde{\ell}} \quad V_{\tilde{\ell}}^\dagger \quad B_{\tilde{\ell}+1} \\ \text{---} \text{---} \text{---} \end{array} = \begin{array}{c} A_{\tilde{\ell}} \quad C_{\tilde{\ell}+1} \\ \text{---} \text{---} \end{array}.$$

Here  $U_{\tilde{\ell}-1}$ ,  $V_{\tilde{\ell}}^\dagger$ ,  $S_{\tilde{\ell}-1}$ ,  $S_{\tilde{\ell}}$  are square matrices, the former two unitary, the latter two diagonal and containing SVD singular values. (Shifting can be combined with truncation, if desired, by discarding some small singular values and correspondingly reducing the bond dimension.) By renaming  $V_{\tilde{\ell}}^\dagger B_{\tilde{\ell}+1}$  as  $B_{\tilde{\ell}+1}$  and defining  $\Lambda_{\tilde{\ell}} = S_{\tilde{\ell}}$ , we can also express  $\Psi^\sigma$  in “bond-canonical” form w.r.t. bond  $\tilde{\ell}$ :

$$\begin{array}{c} A_1 \quad A_{\tilde{\ell}-1} \quad A_{\tilde{\ell}} \quad \Lambda_{\tilde{\ell}} \quad B_{\tilde{\ell}+1} \quad B_{\mathcal{L}} \\ \text{---} \text{---} \text{---} \text{---} \text{---} \text{---} \end{array} \quad (8)$$

The fact that the same MPS can be written in many different but equivalent ways reflects the gauge freedom of MPS representations.

### B. Kept spaces

Given an MPS  $|\Psi\rangle$  in canonical form, its constituent tensors can be used to define a set of state spaces defined on parts of the chain, and a sequence of isometric maps between these state spaces. Let us make this explicit to reveal the underlying structures.

The  $A_{\tilde{\ell}}$  tensors for sites 1 to  $\tilde{\ell}$  can be used to define a set of left *kept* ( $\kappa$ ) states  $|\Psi_{\tilde{\ell}\alpha}^\kappa\rangle$ , and the  $B_{\tilde{\ell}'}$  tensors for sites  $\tilde{\ell}'$  to  $\mathcal{L}$  can be used to define right  $\kappa$  states  $|\Phi_{\tilde{\ell}'\alpha'}^\kappa\rangle$ , with wavefunctions of the form

$$\Psi_{\tilde{\ell}\alpha}^\kappa = \begin{array}{c} A_1 \quad A_{\tilde{\ell}} \\ \text{---} \text{---} \end{array} \alpha, \quad \Phi_{\tilde{\ell}'\alpha'}^\kappa = \begin{array}{c} B_{\tilde{\ell}'} \quad B_{\mathcal{L}} \\ \text{---} \text{---} \end{array} \alpha'. \quad (9)$$

These states are called *kept*, since they are building blocks of  $|\Psi\rangle$ . Their spans define left and right  $\kappa$  spaces,

$$\mathbb{V}_{\tilde{\ell}}^\kappa = \text{span}\{|\Psi_{\tilde{\ell}\alpha}^\kappa\rangle\} \subset \mathbb{V}_1 \otimes \dots \otimes \mathbb{V}_{\tilde{\ell}}, \quad (10)$$

$$\mathbb{W}_{\tilde{\ell}'}^\kappa = \text{span}\{|\Phi_{\tilde{\ell}'\alpha'}^\kappa\rangle\} \subset \mathbb{V}_{\tilde{\ell}'} \otimes \dots \otimes \mathbb{V}_{\mathcal{L}}, \quad (11)$$

of dimension  $D_{\tilde{\ell}}$  and  $D_{\tilde{\ell}'-1}$ , respectively. The dummy sites 0 and  $\mathcal{L}+1$  are represented by one-dimensional spaces,  $\mathbb{V}_0^\kappa$  and  $\mathbb{W}_{\mathcal{L}+1}^\kappa$ .

Each  $A_{\tilde{\ell}}$  and  $B_{\tilde{\ell}'}$  tensor defines an isometric map, from a *parent* (P) space involving a direct product of a  $\kappa$  space and a local space, to an adjacent  $\kappa$  space:

$$A_{\tilde{\ell}}: \mathbb{V}_{\tilde{\ell}-1}^\kappa \otimes \mathbb{V}_{\tilde{\ell}} \rightarrow \mathbb{V}_{\tilde{\ell}}^\kappa, \quad |\Psi_{\tilde{\ell}-1,\alpha}^\kappa\rangle |\sigma_{\tilde{\ell}}\rangle [A_{\tilde{\ell}}]_{\alpha\alpha'}^{\sigma_{\tilde{\ell}}} = |\Psi_{\tilde{\ell}\alpha'}^\kappa\rangle,$$

$$B_{\tilde{\ell}'}: \mathbb{V}_{\tilde{\ell}'} \otimes \mathbb{W}_{\tilde{\ell}'+1}^\kappa \rightarrow \mathbb{W}_{\tilde{\ell}'}^\kappa, \quad [B_{\tilde{\ell}'}]_{\alpha'\alpha'}^{\sigma_{\tilde{\ell}'}} |\Phi_{\tilde{\ell}'+1,\alpha'}^\kappa\rangle = |\Phi_{\tilde{\ell}'\alpha'}^\kappa\rangle.$$

(To connect sites 1 and  $\mathcal{L}$  to their neighboring dummy sites, we define  $\Psi_{0,1}^\kappa = 1$ ,  $\Phi_{\mathcal{L}+1,1}^\kappa = 1$ .) We orient the triangles depicting  $A_{\tilde{\ell}}$  and  $B_{\tilde{\ell}'}$  such that equal-length legs point to parent spaces and 90-degree angles to kept spaces. The dimensions of left or right kept and parent spaces satisfy  $D_{\tilde{\ell}} \leq D_{\tilde{\ell}-1}d$  or  $D_{\tilde{\ell}'} \leq dD_{\tilde{\ell}'}$ , respectively. If a kept space is smaller than its parent space, it has an orthogonal complement, called *discarded* (D) space, discussed in Sec. IID below. The fact that the maps  $A_{\tilde{\ell}}$  and  $B_{\tilde{\ell}'}$  are *isometries* follows from Eqs. (6). These ensure that the left and right  $\kappa$  basis states form orthonormal sets,

$$\langle \Psi_{\tilde{\ell}\alpha}^\kappa | \Psi_{\tilde{\ell}\alpha'}^\kappa \rangle = [\mathbb{1}_{\tilde{\ell}}^\kappa]_{\alpha\alpha'}, \quad \langle \Phi_{\tilde{\ell}'\alpha'}^\kappa | \Phi_{\tilde{\ell}'\alpha''}^\kappa \rangle = [\mathbb{1}_{\tilde{\ell}'-1}^\kappa]_{\alpha'\alpha''},$$

$$\begin{array}{c} \text{---} \text{---} \end{array} = \begin{array}{c} \text{---} \end{array} \mathbb{1}_{\tilde{\ell}}^\kappa, \quad \begin{array}{c} \text{---} \text{---} \end{array} = \begin{array}{c} \text{---} \end{array} \mathbb{1}_{\tilde{\ell}'-1}^\kappa. \quad (12)$$

The basis states can be used to build projectors onto the left or right  $\kappa$  spaces  $\mathbb{V}_{\tilde{\ell}}^\kappa$  or  $\mathbb{W}_{\tilde{\ell}'}^\kappa$ , depicted as

$$\mathcal{P}_{\tilde{\ell}}^\kappa = \sum_{\alpha} |\Psi_{\tilde{\ell}\alpha}^\kappa\rangle \langle \Psi_{\tilde{\ell}\alpha}^\kappa| = \begin{array}{c} \text{---} \text{---} \end{array}, \quad (13a)$$

$$\mathcal{Q}_{\tilde{\ell}'}^\kappa = \sum_{\alpha'} |\Phi_{\tilde{\ell}'\alpha'}^\kappa\rangle \langle \Phi_{\tilde{\ell}'\alpha'}^\kappa| = \begin{array}{c} \text{---} \text{---} \end{array}, \quad (13b)$$

with  $\mathcal{P}_0^\kappa = 1$ ,  $\mathcal{Q}_{\mathcal{L}+1}^\kappa = 1$ , and  $(\mathcal{P}_{\tilde{\ell}}^\kappa)^2 = \mathcal{P}_{\tilde{\ell}}^\kappa$ ,  $(\mathcal{Q}_{\tilde{\ell}'}^\kappa)^2 = \mathcal{Q}_{\tilde{\ell}'}^\kappa$ :

$$\begin{array}{c} \text{---} \text{---} \end{array} = \begin{array}{c} \text{---} \end{array}, \quad \begin{array}{c} \text{---} \text{---} \end{array} = \begin{array}{c} \text{---} \end{array}. \quad (14)$$

### C. Bond, 1s and 2s projectors

The above projectors can, in turn, be used to construct bond, 1s and 2s projectors acting on the full chain,

$$\mathcal{P}_\ell^b = \mathcal{P}_\ell^\kappa \otimes \mathcal{Q}_{\ell+1}^\kappa = \begin{array}{c} \text{---} \text{---} \end{array}, \quad (15a)$$

$$\mathcal{P}_\ell^{1s} = \mathcal{P}_{\ell-1}^\kappa \otimes \mathbb{1}_d \otimes \mathcal{Q}_{\ell+1}^\kappa = \begin{array}{c} \text{---} \text{---} \end{array}, \quad (15b)$$

$$\mathcal{P}_\ell^{2s} = \mathcal{P}_{\ell-1}^\kappa \otimes \mathbb{1}_d \otimes \mathbb{1}_d \otimes \mathcal{Q}_{\ell+2}^\kappa = \begin{array}{c} \text{---} \text{---} \end{array}, \quad (15c)$$

defined for  $\ell \in [0, \mathcal{L}]$ ,  $\ell \in [1, \mathcal{L}]$  and  $\ell \in [1, \mathcal{L}-1]$ , respectively. They mutually commute and satisfy  $(\mathcal{P}_\ell^\kappa)^2 = \mathcal{P}_\ell^\kappa$ , as follows from Eqs. (12) and (14). For example:

$$(\mathcal{P}_\ell^b)^2 = \begin{array}{c} \text{---} \text{---} \end{array} = \begin{array}{c} \text{---} \end{array} = \mathcal{P}_\ell^b.$$

The projectors  $\mathcal{P}^b$ ,  $\mathcal{P}^{1s}$  and  $\mathcal{P}^{2s}$  map the full  $\mathbb{V}$  into the subspaces  $\mathbb{V}_\ell^K \otimes \mathbb{W}_{\ell+1}^K$ ,  $\mathbb{V}_{\ell-1}^K \otimes \mathbb{v}_\ell \otimes \mathbb{W}_{\ell+1}^K$  and  $\mathbb{V}_{\ell-1}^K \otimes \mathbb{v}_\ell \otimes \mathbb{v}_{\ell+1} \otimes \mathbb{W}_{\ell+2}^K$ . These spaces offer three equivalent representations of the same state  $|\Psi\rangle$ , in bond-, 1s- or 2s-canonical form,

$$|\Psi\rangle = |\Psi_{\ell\alpha}^K\rangle |\Phi_{\ell+1,\alpha'}^K\rangle [\psi_\ell^b]_{\alpha\alpha'} \quad (16a)$$

$$= |\Psi_{\ell-1,\alpha}^K\rangle |\sigma_\ell\rangle |\Phi_{\ell+1,\alpha'}^K\rangle [\psi_\ell^{1s}]_{\alpha\alpha'}^{\sigma_\ell} \quad (16b)$$

$$= |\Psi_{\ell-1,\alpha}^K\rangle |\sigma_\ell\rangle |\sigma_{\ell+1}\rangle |\Phi_{\ell+2,\alpha'}^K\rangle [\psi_\ell^{2s}]_{\alpha\alpha'}^{\sigma_\ell\sigma_{\ell+1}}, \quad (16c)$$

$$\psi_\ell^b = \Lambda_\ell, \quad \psi_\ell^{1s} = C_\ell, \quad \psi_\ell^{2s} = A_\ell \Lambda_\ell B_{\ell+1}. \quad (16d)$$

These forms emphasize the tensors describing bond  $\ell$ , site  $\ell$  or sites  $(\ell, \ell+1)$  and the bond in between, respectively. For example, Eqs. (16a) and (16b) are depicted as

$$\Psi = \underbrace{A_1 \dots A_\ell}_{\Psi_{\ell\alpha}^K} \underbrace{\Lambda_\ell B_{\ell+1}}_{\Phi_{\ell+1,\alpha'}^K} B_{\mathcal{L}} = \underbrace{A_1 \dots A_{\ell-1}}_{\Psi_{\ell-1,\alpha}^K} \underbrace{C_\ell}_{\sigma_\ell} \underbrace{B_{\ell+1} B_{\mathcal{L}}}_{\Phi_{\ell+1,\alpha'}^K}.$$

The projections of the Hamiltonian into these spaces,  $\mathcal{H}_\ell^\times = \mathcal{P}_\ell^\times \mathcal{H} \mathcal{P}_\ell^\times$ , have matrix elements of the form

$$H_\ell^b = \left[ \begin{array}{c} \text{---} \text{---} \text{---} \\ \ell \quad \ell+1 \end{array} \right], \quad H_\ell^{1s} = \left[ \begin{array}{c} \text{---} \text{---} \text{---} \\ \ell-1 \quad \ell \quad \ell+1 \end{array} \right], \quad H_\ell^{2s} = \left[ \begin{array}{c} \text{---} \text{---} \text{---} \\ \ell-1 \quad \ell \quad \ell+1 \quad \ell+2 \end{array} \right], \quad (17)$$

with left and right environments for sites  $\ell \pm 1$  given by

$$L_\ell = \left[ \begin{array}{c} \text{---} \text{---} \text{---} \\ \ell \end{array} \right] = \left[ \begin{array}{c} \text{---} \text{---} \text{---} \\ 1 \quad \ell \end{array} \right] = \left[ \begin{array}{c} \text{---} \text{---} \text{---} \\ L_{\ell-1} \quad \ell \end{array} \right], \quad (18a)$$

$$R_\ell = \left[ \begin{array}{c} \text{---} \text{---} \text{---} \\ \ell \end{array} \right] = \left[ \begin{array}{c} \text{---} \text{---} \text{---} \\ \ell \quad \mathcal{L} \end{array} \right] = \left[ \begin{array}{c} \text{---} \text{---} \text{---} \\ \ell \quad R_{\ell+1} \end{array} \right]. \quad (18b)$$

Here the first equalities define  $L_\ell$  and  $R_\ell$ , the second equalities show how they can be computed recursively, starting from  $L_0 = 1$ ,  $R_{\mathcal{L}+1} = 1$ . The open triangles on  $L_\ell$  and  $R_\ell$  signify that they are computed using left- or right-normalized  $A$  or  $B$  tensors.

The above matrix elements are standard ingredients in numerous MPS algorithms. To give a specific example, we briefly recall their role in DMRG ground state searches. These seek approximate ground state solutions to  $\mathcal{H}|\Psi\rangle = E|\Psi\rangle$  through a sequence of local optimization steps. Focusing on bond  $\ell$ , or site  $\ell$ , or sites  $(\ell, \ell+1)$ , one updates  $\Lambda_\ell$ , or  $C_\ell$ , or  $A_\ell \Lambda_\ell B_{\ell+1}$ , by finding the ground state solution of, respectively,

$$(H_\ell^b - E)\psi_\ell^b = 0, \quad \left[ \begin{array}{c} \text{---} \text{---} \text{---} \\ \ell \quad \ell+1 \end{array} \right] = E \text{---} \text{---} \text{---}, \quad (19a)$$

$$(H_\ell^{1s} - E)\psi_\ell^{1s} = 0, \quad \left[ \begin{array}{c} \text{---} \text{---} \text{---} \\ \ell-1 \quad \ell \quad \ell+1 \end{array} \right] = E \text{---} \text{---} \text{---}, \quad (19b)$$

$$(H_\ell^{2s} - E)\psi_\ell^{2s} = 0, \quad \left[ \begin{array}{c} \text{---} \text{---} \text{---} \\ \ell-1 \quad \ell \quad \ell+1 \quad \ell+2 \end{array} \right] = E \text{---} \text{---} \text{---}. \quad (19c)$$

One then uses Eq. (7) to shift the orthogonality center to the neighboring bond or site, optimizes it, and sweeps

back and forth through the chain until the ground state energy has converged. These three schemes are known as 0s or bond DMRG, 1s and 2s DMRG, respectively. They differ regarding their flexibility for increasing (“expanding”) virtual bond dimensions, which increases the size of the variational space and hence the accuracy of the converged ground state energy. 0s and 1s DMRG offer no way of doing this, because the tensors  $\Lambda_\ell$  or  $C_\ell$  have the same dimensions after the update as before. By contrast, 2s DMRG does offer a way of expanding bond dimensions: the bonds connecting the updated tensors  $A_\ell$ ,  $\Lambda_\ell$  and  $B_{\ell+1}$  have dimensions  $d \min(D_{\ell-1}, D_{\ell+1})$ , which is  $\geq D_\ell$ ; one may thus expand bond  $\ell$  by retaining more than  $D_\ell$  singular values in  $\Lambda_\ell$ . However, this comes at a price. The numerical cost is  $\mathcal{O}(D^3 d^2 w)$  for applying  $H^{2s}$  to  $\psi^{2s}$  during the iterative solution of the eigenvalue problem Eq. (19c), and  $\mathcal{O}(D^3 d^3)$  for SVDing the resulting eigenstate to identify the updated  $A$ ,  $\Lambda$ , and  $B$ . By contrast, for 1s DMRG the costs are lower:  $\mathcal{O}(D^3 d w)$  for applying  $H^{1s}$  to  $C$ , and  $\mathcal{O}(D^3 d)$  for SVDing  $C$  to shift to the next site. Various schemes have been proposed for achieving 2s accuracy at 1s costs, see Refs. [4, 5, 29].

#### D. Discarded spaces

In this section, we define discarded spaces as the orthogonal complements of kept spaces, and introduce their corresponding isometries and discarded space projectors.

As mentioned above, the kept spaces  $\mathbb{V}_\ell^K$  and  $\mathbb{W}_{\ell'}^K$  have dimensions smaller than the parent spaces  $\mathbb{V}_{\ell-1}^K \otimes \mathbb{v}_\ell$  and  $\mathbb{v}_{\ell'} \otimes \mathbb{W}_{\ell'+1}^K$  from which they are constructed. Their orthogonal complements are the above-mentioned discarded spaces, to be denoted  $\mathbb{V}_\ell^D$  and  $\mathbb{W}_{\ell'}^D$ , respectively, of dimension  $\overline{D}_\ell^A = D_{\ell-1}d - D_\ell$  and  $\overline{D}_{\ell'}^B = D_{\ell'}d - D_{\ell'+1}$ . By definition,  $\text{span}\{\mathbb{V}_\ell^K, \mathbb{V}_\ell^D\}$  and  $\text{span}\{\mathbb{W}_{\ell'}^K, \mathbb{W}_{\ell'}^D\}$  yield the full parent spaces, respectively. Let  $\overline{A}_\ell$  and  $\overline{B}_{\ell'}$  be isometries from the parent to the discarded spaces,

$$\overline{A}_\ell: \mathbb{V}_{\ell-1}^K \otimes \mathbb{v}_\ell \rightarrow \mathbb{V}_\ell^D, \quad |\Psi_{\ell-1,\alpha}^K\rangle |\sigma_\ell\rangle [\overline{A}_\ell]_{\alpha\alpha'}^{\sigma_\ell} = |\Psi_{\ell\alpha}^D\rangle, \\ \overline{B}_{\ell'}: \mathbb{v}_{\ell'} \otimes \mathbb{W}_{\ell'+1}^K \rightarrow \mathbb{W}_{\ell'}^D, \quad [\overline{B}_{\ell'}]_{\alpha\alpha'}^{\sigma_{\ell'}} |\sigma_{\ell'}\rangle |\Phi_{\ell'+1,\alpha'}^K\rangle = |\Phi_{\ell'\alpha}^D\rangle.$$

Then  $A_\ell \oplus \overline{A}_\ell$  and  $B_{\ell'} \oplus \overline{B}_{\ell'}$  are unitary maps on the parent spaces, and Eq. (6) is complemented by relations expressing orthonormality and completeness:

$$\overline{A}_\ell^\dagger \overline{A}_\ell = \mathbb{1}_\ell^D, \quad A_\ell^\dagger \overline{A}_\ell = 0, \quad \overline{B}_{\ell'}^\dagger \overline{B}_{\ell'} = \mathbb{1}_{\ell'-1}^D, \quad \overline{B}_{\ell'}^\dagger B_{\ell'} = 0, \\ \left[ \begin{array}{c} \text{---} \text{---} \text{---} \\ \ell \end{array} \right] = \left[ \begin{array}{c} \text{---} \text{---} \text{---} \\ \ell \end{array} \right] = \mathbb{1}_\ell^D, \quad \left[ \begin{array}{c} \text{---} \text{---} \text{---} \\ \ell \end{array} \right] = 0, \quad \left[ \begin{array}{c} \text{---} \text{---} \text{---} \\ \ell' \end{array} \right] = \mathbb{1}_{\ell'-1}^D, \quad \left[ \begin{array}{c} \text{---} \text{---} \text{---} \\ \ell' \end{array} \right] = 0, \quad (20)$$

$$A_\ell A_\ell^\dagger + \overline{A}_\ell \overline{A}_\ell^\dagger = \mathbb{1}_\ell^P, \quad B_{\ell'}^\dagger B_{\ell'} + \overline{B}_{\ell'}^\dagger \overline{B}_{\ell'} = \mathbb{1}_{\ell'-1}^P, \\ \left[ \begin{array}{c} \text{---} \text{---} \text{---} \\ \ell \end{array} \right] + \left[ \begin{array}{c} \text{---} \text{---} \text{---} \\ \ell \end{array} \right] = \left| \begin{array}{c} \text{---} \text{---} \text{---} \\ \ell \end{array} \right| = \mathbb{1}_\ell^P, \quad \left[ \begin{array}{c} \text{---} \text{---} \text{---} \\ \ell' \end{array} \right] + \left[ \begin{array}{c} \text{---} \text{---} \text{---} \\ \ell' \end{array} \right] = \left| \begin{array}{c} \text{---} \text{---} \text{---} \\ \ell' \end{array} \right| = \mathbb{1}_{\ell'-1}^P. \quad (21)$$

Here, left- or right-oriented grey triangles denote the complements  $\overline{A}_\ell$  and  $\overline{B}_{\ell'}$  associated with discarded spaces.



The orthogonality relations (6) and (20) state that  $\kappa$  meeting  $\kappa$  or  $\mathcal{D}$  meeting  $\mathcal{D}$  yield unity, whereas  $\kappa$  meeting  $\mathcal{D}$  yields zero. We will use them often below. For the completeness relations (21),  $\mathbb{1}_\ell^P = \mathbb{1}_{\ell-1}^\kappa \otimes \mathbb{1}_d$  and  $\mathbb{1}_{\ell'-1}^P = \mathbb{1}_d \otimes \mathbb{1}_{\ell'}^\kappa$  are identity matrices on the parent spaces, with  $\mathbb{1}_d$  a  $d \times d$  unit matrix. In numerical practice, it is desirable to avoid the explicit computation of  $\bar{A}_\ell \bar{A}_\ell^\dagger$  or  $\bar{B}_{\ell'}^\dagger \bar{B}_{\ell'}$ , since these are huge objects. Instead, one can always use Eq. (21) to express them as  $\mathbb{1}_\ell^P - A_\ell A_\ell^\dagger$  or  $\mathbb{1}_{\ell'-1}^P - B_{\ell'}^\dagger B_{\ell'}$ .

Equations (21) imply additional identities that will likewise be useful below:

$$\circlearrowleft|_c = \circlearrowleft|_c + \circlearrowleft|_c = \circlearrowleft|_c + \circlearrowleft|_c, \quad (22a)$$

$$\circlearrowleft|_c|_{c+1} = \circlearrowleft|_c|_{c+1} + \circlearrowleft|_c|_{c+1} + \circlearrowleft|_c|_{c+1} + \circlearrowleft|_c|_{c+1}, \quad (22b)$$

$$\circlearrowleft|_c|_{c+1} = \circlearrowleft|_c|_{c+1} - \circlearrowleft|_c|_{c+1} - \circlearrowleft|_c|_{c+1} + \circlearrowleft|_c|_{c+1}. \quad (22c)$$

The first two lines can be used to express 1s or 2s projectors through bond projectors, as elaborated below. The third line follows from the first two. The two equivalent forms on the right of Eq. (22a) arise from combining the physical state space of site  $\ell$  with virtual state spaces on either the left or the right, yielding either left- or right-normalized parent spaces.

In complete analogy to Eqs. (9) to (13), the complement isometries can be used to define orthonormal bases states for the left and right discarded spaces  $\mathbb{W}_\ell^D$  and  $\mathbb{W}_{\ell'}^D$ ,

$$\Psi_{\ell\alpha}^D = \begin{array}{c} A_1 \\ \circlearrowleft \\ \circlearrowleft \\ \circlearrowleft \end{array} \bar{A}_\ell \alpha, \quad \Phi_{\ell'\alpha'}^D = \alpha' \begin{array}{c} \bar{B}_{\ell'} \\ \circlearrowleft \\ \circlearrowleft \\ \circlearrowleft \end{array} B_{\ell'}, \quad (23)$$

satisfying the orthonormality relations

$$\begin{array}{c} \circlearrowleft \\ \circlearrowleft \\ \circlearrowleft \end{array} \begin{array}{c} \circlearrowleft \\ \circlearrowleft \\ \circlearrowleft \end{array} = \begin{pmatrix} \circlearrowleft \\ \circlearrowleft \\ \circlearrowleft \end{pmatrix}, \quad \begin{array}{c} \circlearrowleft \\ \circlearrowleft \\ \circlearrowleft \end{array} \begin{array}{c} \circlearrowleft \\ \circlearrowleft \\ \circlearrowleft \end{array} = \begin{pmatrix} \circlearrowleft \\ \circlearrowleft \\ \circlearrowleft \end{pmatrix}, \quad (24a)$$

$$\begin{array}{c} \circlearrowleft \\ \circlearrowleft \\ \circlearrowleft \end{array} \begin{array}{c} \circlearrowleft \\ \circlearrowleft \\ \circlearrowleft \end{array} = 0, \quad \begin{array}{c} \circlearrowleft \\ \circlearrowleft \\ \circlearrowleft \end{array} \begin{array}{c} \circlearrowleft \\ \circlearrowleft \\ \circlearrowleft \end{array} = 0. \quad (24b)$$

The corresponding projectors are defined as

$$\mathcal{P}_\ell^D = \sum_\alpha |\Psi_{\ell\alpha}^D\rangle\langle\Psi_{\ell\alpha}^D| = \begin{array}{c} \circlearrowleft \\ \circlearrowleft \\ \circlearrowleft \end{array}, \quad (25)$$

$$\mathcal{Q}_{\ell'}^D = \sum_{\alpha'} |\Phi_{\ell'\alpha'}^D\rangle\langle\Phi_{\ell'\alpha'}^D| = \begin{array}{c} \circlearrowleft \\ \circlearrowleft \\ \circlearrowleft \end{array}, \quad (26)$$

with  $\mathcal{P}_0^D = \mathcal{Q}_{\mathcal{L}+1}^D = 0$ . They obey orthonormality relations,

$$\mathcal{P}_\ell^x \mathcal{P}_\ell^{\bar{x}} = \delta^{x\bar{x}} \mathcal{P}_\ell^x, \quad \mathcal{Q}_{\ell'}^x \mathcal{Q}_{\ell'}^{\bar{x}} = \delta^{x\bar{x}} \mathcal{Q}_{\ell'}^x, \quad (27)$$

where here and henceforth,  $x, \bar{x} \in \{\kappa, \mathcal{D}\}$ . Moreover, Eq. (21) implies the completeness relations

$$\mathcal{P}_\ell^\kappa + \mathcal{P}_\ell^\mathcal{D} = \mathcal{P}_{\ell-1}^\kappa \otimes \mathbb{1}_d, \quad \mathcal{Q}_{\ell'}^\kappa + \mathcal{Q}_{\ell'}^\mathcal{D} = \mathbb{1}_d \otimes \mathcal{Q}_{\ell'+1}^\kappa, \quad (28)$$

stating that the kept and discarded projectors of a given site together form a projector for their parent space. These will play a crucial role in subsequent sections.

To conclude this section, we apply the projector identity (22b) to the open legs of the state  $\mathcal{H}_\ell^{2s} \psi_\ell^{2s}$  appearing in the 2s Schrödinger (19c). We obtain:

$$\begin{array}{c} \ell-1 \quad \ell \quad \ell+1 \quad \ell+2 \\ \circlearrowleft \quad \circlearrowleft \quad \circlearrowleft \quad \circlearrowleft \end{array} + \begin{array}{c} \ell \quad \ell+1 \\ \circlearrowleft \quad \circlearrowleft \end{array} + \begin{array}{c} \ell \quad \ell+1 \\ \circlearrowleft \quad \circlearrowleft \end{array} + \begin{array}{c} \ell \quad \ell+1 \\ \circlearrowleft \quad \circlearrowleft \end{array}, \\ = \begin{array}{c} \ell \quad \ell+1 \\ \circlearrowleft \quad \circlearrowleft \end{array} + \begin{array}{c} \ell \quad \ell+1 \\ \circlearrowleft \quad \circlearrowleft \end{array} + \begin{array}{c} \ell \quad \ell+1 \\ \circlearrowleft \quad \circlearrowleft \end{array} + \begin{array}{c} \ell \quad \ell+1 \\ \circlearrowleft \quad \circlearrowleft \end{array}. \quad (29)$$

If only the first term is retained, the 2s Schrödinger Eq. (19c) reduces to the bond Schrödinger Eq. (19a), sandwiched between  $A_\ell$  and  $B_{\ell+1}$ :

$$A_\ell (H_\ell^b - E) \Lambda_\ell B_{\ell+1} = 0. \quad (30a)$$

The first term together with the second or third term reduces to the 1s Schrödinger Eq. (19b) for sites  $\ell+1$  or  $\ell$ , left- or right-contracted with  $A_\ell$  and  $B_{\ell+1}$ , respectively:

$$A_\ell (H_{\ell+1}^{1s} - E) C_{\ell+1} = 0 \quad (30b)$$

$$(H_\ell^{1s} - E) C_\ell B_{\ell+1} = 0. \quad (30c)$$

All four terms together of course give the full 2s Schrödinger Eq. (19c),

$$(H_\ell^{2s} - E) A_\ell \Lambda_\ell B_{\ell+1} = 0. \quad (30d)$$

Evidently, the fourth term in Eq. (29), involving a DD projector pair, is beyond the reach of 1s schemes. A strategy for nevertheless computing its most important contributions with 1s costs, called controlled bond expansion, has recently been formulated by us in Ref. [29].

### III. CONSTRUCTION OF $\mathcal{P}^{ns}$ AND $\mathcal{P}^{n\perp}$

As discussed in the introduction, each site of an MPS  $|\Psi\rangle$  induces a splitting of the local Hilbert space into  $\kappa$  and  $\mathcal{D}$  sectors. This induces a partition of the full vector space  $\mathbb{V}$  into intricately nested orthogonal subspaces [6]. It is useful to identify orthogonal projectors for these subspaces. Gauge invariance—the existence of many equivalent representations of  $|\Psi\rangle$ —makes this a nontrivial task. It can be accomplished systematically by Gram-Schmidt orthogonalization, formulated in projector language. The following three sections are devoted to this endeavor.

In the present section, we define a set of projectors,  $\mathcal{P}_{\ell\bar{\ell}}^{x\bar{x}}$ ,  $x, \bar{x} \in \{\kappa, \mathcal{D}\}$ , involving kept and/or discarded sectors at sites  $\ell, \bar{\ell}$ . These serve as building blocks for all projectors introduced thereafter. Then, in Sec. III B, we define generalized local  $n$ -site ( $ns$ ) projectors,  $\mathcal{P}_\ell^{ns}$ , describing variations of  $|\Psi\rangle$  involving up to  $n$  contiguous

sites. In Sec. III C, we add them up to obtain *global ns* projectors,  $\mathcal{P}^{ns}$ ; and in Sec. III D we orthogonalize these to obtain *irreducible global ns* projectors,  $\mathcal{P}^{n\perp}$ , not expressible through combinations of variations on subsets of  $n' < n$  sites. They are useful for various purposes, including the computation of the energy variance [6], and the formulation of MPS algorithms based on the notion of tangent spaces [11–14, 30] and generalizations thereof. Throughout, we concisely summarize the properties of the various projectors encountered along the way.

### A. Projectors for kept and discarded sectors, $\mathcal{P}_{\ell\bar{\ell}}^{x\bar{x}}$

We start by introducing kept and discarded space projectors defined on the full Hilbert space  $\mathbb{V}$ . To this end, we supplement  $\mathcal{P}_{\ell}^x$  and  $\mathcal{Q}_{\ell}^x$  by right or left environments (E) comprising the entire rest of the chain, and define

$$\mathcal{P}_{\ell}^{xE} = \mathcal{P}_{\ell}^x \otimes \mathbb{1}_d^{\otimes \mathcal{L}-\ell}, \quad \mathcal{P}_{\ell}^{EX} = \mathbb{1}_d^{\otimes \ell-1} \otimes \mathcal{Q}_{\ell}^x, \quad (31)$$

$$\begin{aligned} \mathcal{P}_{\ell}^{KE} &= \text{diagram with } \mathcal{P}_{\ell}^K \text{ and } \mathbb{1}_d^{\otimes \mathcal{L}-\ell} \text{ on the right}, & \mathcal{P}_{\ell}^{EK} &= \text{diagram with } \mathbb{1}_d^{\otimes \ell-1} \text{ and } \mathcal{Q}_{\ell}^K \text{ on the left}, \\ \mathcal{P}_{\ell}^{DE} &= \text{diagram with } \mathcal{P}_{\ell}^D \text{ and } \mathbb{1}_d^{\otimes \mathcal{L}-\ell} \text{ on the right}, & \mathcal{P}_{\ell}^{ED} &= \text{diagram with } \mathbb{1}_d^{\otimes \ell-1} \text{ and } \mathcal{Q}_{\ell}^D \text{ on the left}. \end{aligned}$$

with  $\ell \in [0, \mathcal{L}]$  for  $\mathcal{P}_{\ell}^{xE}$  and  $\ell \in [1, \mathcal{L}+1]$  for  $\mathcal{P}_{\ell}^{EX}$ . Equations (12) and (24) imply orthogonality relations for projectors with E on the same side (both right or both left):

$$\mathcal{P}_{\ell}^{xE} \mathcal{P}_{\bar{\ell}}^{\bar{x}\bar{E}} = \delta^{\ell < \bar{\ell}} \delta_{x\bar{x}} \mathcal{P}_{\ell}^{\bar{x}\bar{E}} + \delta^{\ell\bar{\ell}} \delta_{x\bar{x}} \mathcal{P}_{\ell}^{\bar{x}\bar{E}} + \delta^{\ell > \bar{\ell}} \mathcal{P}_{\ell}^{xE} \delta_{x\bar{x}}, \quad (32a)$$

$$\mathcal{P}_{\ell}^{EX} \mathcal{P}_{\bar{\ell}}^{\bar{E}\bar{x}} = \delta^{\ell < \bar{\ell}} \mathcal{P}_{\ell}^{EX} \delta_{x\bar{x}} + \delta^{\ell\bar{\ell}} \delta_{x\bar{x}} \mathcal{P}_{\ell}^{\bar{E}\bar{x}} + \delta^{\ell > \bar{\ell}} \delta_{x\bar{x}} \mathcal{P}_{\bar{\ell}}^{\bar{E}\bar{x}}. \quad (32b)$$

The  $\delta$  symbols indicate that the first, second, and third terms contribute only for  $\ell < \bar{\ell}$ ,  $\ell = \bar{\ell}$ , and  $\ell > \bar{\ell}$ , respectively. Thus, same-site projectors are orthonormal; different-site products with Es on the same side, of the type  $\mathcal{P}_{\ell}^{xE} \mathcal{P}_{\bar{\ell}}^{\bar{x}\bar{E}}$  (or  $\mathcal{P}_{\ell}^{EX} \mathcal{P}_{\bar{\ell}}^{\bar{E}\bar{x}}$ ), vanish if the earlier (later) site hosts a D; if it hosts a K, they yield the projector from the other site. We depict two cases of Eq. (32a) below:

$$\begin{aligned} \mathcal{P}_{\ell}^{DE} \mathcal{P}_{\bar{\ell}}^{DE} &= \text{diagram with two D projectors on the same side} = \text{diagram with one D projector on the other side} = \mathcal{P}_{\bar{\ell}}^{DE}, \\ \mathcal{P}_{\ell}^{KE} \mathcal{P}_{\bar{\ell}}^{DE} &= \text{diagram with K and D projectors on the same side} = \text{diagram with one D projector on the other side} = \mathcal{P}_{\bar{\ell}}^{DE}. \end{aligned}$$

Equation (32a) was first written down in that form in Ref. [27], Eq. (29), in the context of NRG. There, one deals exclusively with left-normalized states, and sites to the right of the orthogonality center are treated purely as environmental degrees of freedom, described by product states. Equation (32b) is the counterpart of (32a) for right-normalized states.

Projector products with Es in the middle,  $\mathcal{P}_{\ell}^{xE} \mathcal{P}_{\bar{\ell}}^{\bar{x}\bar{E}}$ , and  $\ell < \bar{\ell}$ , again yield projectors. We denote them by

$$\mathcal{P}_{\ell\bar{\ell}}^{x\bar{x}} = \mathcal{P}_{\ell}^{xE} \mathcal{P}_{\bar{\ell}}^{\bar{x}\bar{E}} \quad (0 \leq \ell < \bar{\ell} \leq \mathcal{L}+1), \quad (33)$$

$$\begin{aligned} \mathcal{P}_{\ell\bar{\ell}}^{KK} &= \text{diagram with two K projectors on the same side}, & \mathcal{P}_{\ell\bar{\ell}}^{KD} &= \text{diagram with K and D projectors on the same side}, \\ \mathcal{P}_{\ell\bar{\ell}}^{DK} &= \text{diagram with D and K projectors on the same side}, & \mathcal{P}_{\ell\bar{\ell}}^{DD} &= \text{diagram with two D projectors on the same side}. \end{aligned}$$

They have local unit operators on  $n = \bar{\ell} - (\ell + 1)$  contiguous sites, sandwiched between any combination of K and D projectors to the left and right. In this sense, they generalize Eqs. (15) and will be called generalized *local ns* projectors. They fulfill numerous orthogonality relations following directly from Eqs. (32). For example:

$$\mathcal{P}_{\ell\bar{\ell}}^{x\bar{x}} \mathcal{P}_{\ell'\bar{\ell}'}^{x'\bar{x}'} = \delta^{xx'} \delta^{\bar{x}\bar{x}'} \mathcal{P}_{\ell\bar{\ell}}^{x\bar{x}}, \quad (34a)$$

$$\forall \ell < \ell': \mathcal{P}_{\ell\bar{\ell}}^{x\bar{x}} \mathcal{P}_{\ell'\bar{\ell}'}^{x'\bar{x}'} = 0, \quad \forall \bar{\ell} < \bar{\ell}': \mathcal{P}_{\ell\bar{\ell}}^{x\bar{x}} \mathcal{P}_{\ell'\bar{\ell}'}^{x'\bar{x}'} = 0, \quad (34b)$$

$$\mathcal{P}_{\ell\bar{\ell}}^{D\bar{D}} \mathcal{P}_{\ell'\bar{\ell}'}^{D'\bar{D}'} \sim \delta_{\ell\ell'}, \quad \mathcal{P}_{\ell\bar{\ell}}^{x\bar{x}} \mathcal{P}_{\ell'\bar{\ell}'}^{x'\bar{x}'} \sim \delta_{\bar{\ell}\bar{\ell}'}. \quad (34c)$$

Thus, two projectors having the same site indices are orthonormal; projector products involving a D on a site earlier or later than all other indexed sites vanish; those involving two Ds on the same side but different sites vanish, too. Some of these relations are illustrated below:

$$\begin{aligned} \mathcal{P}_{\ell\bar{\ell}}^{DK} \mathcal{P}_{\ell\bar{\ell}}^{DK} &= \text{diagram with two DK projectors on the same side} = \text{diagram with one DK projector on the other side} = \mathcal{P}_{\ell\bar{\ell}}^{DK}, \\ \mathcal{P}_{\ell\bar{\ell}}^{DK} \mathcal{P}_{\ell'\bar{\ell}'}^{KK} &= \text{diagram with DK and KK projectors on the same side} = 0, \\ \mathcal{P}_{\ell\bar{\ell}}^{DK} \mathcal{P}_{\ell\bar{\ell}}^{DD} &= \text{diagram with DK and DD projectors on the same side} = \text{diagram with one DD projector on the other side} = \mathcal{P}_{\ell\bar{\ell}}^{DD}. \end{aligned}$$

Eq. (28) implies another useful property (for  $\bar{\ell} - \ell > 1$ ),

$$\mathcal{P}_{\ell\bar{\ell}}^{K\bar{K}} = \mathcal{P}_{\ell+1, \bar{\ell}}^{K\bar{K}} + \mathcal{P}_{\ell+1, \bar{\ell}}^{D\bar{D}}, \quad \mathcal{P}_{\ell\bar{\ell}}^{x\bar{x}} = \mathcal{P}_{\ell, \bar{\ell}-1}^{x\bar{x}} + \mathcal{P}_{\ell, \bar{\ell}-1}^{x\bar{D}}. \quad (35)$$

reflecting Eq. (22b). Thus, a K on a given site  $\ell$  (or  $\bar{\ell}$ ) can be decomposed into K and D on the inner neighboring site  $\ell+1$  (or  $\bar{\ell}-1$ ), thereby expressing one projector through two that both target one less site. This decomposition will be used repeatedly below.

### B. Local $n$ -site projectors, $\mathcal{P}_{\ell}^{ns}$

The KK projectors merit special attention. For  $\bar{\ell} - \ell = 1$ , 2 or 3, they correspond to the bond, 1s and 2s projectors introduced in Eqs. (15). These can be expressed as

$$\mathcal{P}_{\ell}^b = \mathcal{P}_{\ell, \ell+1}^{KK}, \quad \mathcal{P}_{\ell}^{1s} = \mathcal{P}_{\ell-1, \ell+1}^{KK}, \quad \mathcal{P}_{\ell}^{2s} = \mathcal{P}_{\ell-1, \ell+2}^{KK}. \quad (36)$$

Generalizing the notation of (36), we define a set of local  $ns$  projectors (for  $n \geq 0$  and  $\ell \in [1, \mathcal{L}+1-n]$ ) as:

$$\mathcal{P}_\ell^{ns} = \mathcal{P}_{\ell-1, \ell+n}^{\text{KK}} = \begin{array}{c} \text{\tiny $n$ sites} \\ \begin{array}{c} \text{\tiny $\ell$} \quad \text{\tiny $\ell+1$} \quad \dots \quad \text{\tiny $\ell+n$} \end{array} \end{array} \quad (37)$$

Then  $\mathcal{P}_\ell^{0s} = \mathcal{P}_{\ell-1}^b$ , and for  $n \geq 1$ , these projectors span the spaces of variations of  $|\Psi\rangle$  on  $n$  contiguous sites from  $\ell$  to  $\ell+n-1$ . However, projectors  $\mathcal{P}_\ell^{ns}$  and  $\mathcal{P}_{\ell'}^{ns}$  with  $\ell \neq \ell'$  are not orthogonal. Instead, the following relations hold for all  $\ell < \ell'$ ,

$$\mathcal{P}_\ell^{ns} \mathcal{P}_{\ell'}^{ns} = \mathcal{P}_{\ell+1}^{(n-1)s} \mathcal{P}_{\ell'}^{ns} = \mathcal{P}_\ell^{ns} \mathcal{P}_{\ell'}^{(n-1)s} = \mathcal{P}_{\ell+1}^{(n-1)s} \mathcal{P}_{\ell'}^{(n-1)s}, \quad (38)$$

as can be verified using Eqs. (32). For example, for

$$\begin{aligned} \mathcal{P}_\ell^{ns} \mathcal{P}_{\ell'}^{ns} &= \begin{array}{c} \text{\tiny $\ell'$} \quad \text{\tiny $\ell'+n$} \\ \begin{array}{c} \text{\tiny $\ell$} \quad \text{\tiny $\ell+1$} \quad \dots \quad \text{\tiny $\ell+n$} \end{array} \end{array} = \begin{array}{c} \text{\tiny $\ell'$} \quad \text{\tiny $\ell'+n$} \\ \begin{array}{c} \text{\tiny $\ell$} \quad \text{\tiny $\ell+1$} \quad \dots \quad \text{\tiny $\ell+n$} \end{array} \end{array}, \\ \mathcal{P}_{\ell+1}^{(n-1)s} \mathcal{P}_{\ell'}^{ns} &= \begin{array}{c} \text{\tiny $\ell'$} \quad \text{\tiny $\ell'+n$} \\ \begin{array}{c} \text{\tiny $\ell+1$} \quad \text{\tiny $\ell+2$} \quad \dots \quad \text{\tiny $\ell+n$} \end{array} \end{array} = \begin{array}{c} \text{\tiny $\ell'$} \quad \text{\tiny $\ell'+n$} \\ \begin{array}{c} \text{\tiny $\ell+1$} \quad \text{\tiny $\ell+2$} \quad \dots \quad \text{\tiny $\ell+n$} \end{array} \end{array}, \end{aligned}$$

we obtain the same result in both cases. In particular, for  $n \geq 1$ , two  $ns$  projectors mismatched by one site yield an  $(n-1)$ -site projector,

$$\mathcal{P}_\ell^{ns} \mathcal{P}_{\ell+1}^{ns} = \mathcal{P}_{\ell+1}^{(n-1)s} \quad (39)$$

$$\begin{array}{c} \text{\tiny $\ell+1$} \quad \text{\tiny $\ell+n+1$} \\ \begin{array}{c} \text{\tiny $\ell$} \quad \text{\tiny $\ell+1$} \quad \dots \quad \text{\tiny $\ell+n$} \end{array} \end{array} = \begin{array}{c} \text{\tiny $\ell+1$} \quad \text{\tiny $\ell+n$} \\ \begin{array}{c} \text{\tiny $\ell$} \quad \text{\tiny $\ell+1$} \quad \dots \quad \text{\tiny $\ell+n$} \end{array} \end{array}.$$

Orthogonalized versions of the  $\mathcal{P}_\ell^{ns}$  projectors will be constructed in the next subsection. Here, we collect some properties, following from Eq. (32), that will be needed for that purpose:

$$\forall \ell < \ell': \quad \mathcal{P}_{\ell\ell}^{\text{D}\bar{\text{X}}} \mathcal{P}_{\ell'}^{ns} = 0, \quad (40a)$$

$$\forall (\ell+n) \leq \bar{\ell}': \quad \mathcal{P}_\ell^{ns} \mathcal{P}_{\ell'\bar{\ell}'}^{\text{X}'\text{D}} = 0. \quad (40b)$$

Thus,  $\mathcal{P}_\ell^{ns}$  is annihilated by a left D on its left or a right D on its right. For example,

$$\mathcal{P}_\ell^{ns} \mathcal{P}_{\ell'\bar{\ell}'}^{\text{KD}} = \begin{array}{c} \text{\tiny $\ell'$} \quad \text{\tiny $\bar{\ell}'$} \\ \begin{array}{c} \text{\tiny $\ell$} \quad \text{\tiny $\ell+1$} \quad \dots \quad \text{\tiny $\ell+n$} \end{array} \end{array} = 0.$$

Using Eq. (35),  $\mathcal{P}_\ell^{ns}$  can be expressed through two  $(n-1)s$  projectors:

$$\mathcal{P}_\ell^{ns} = \mathcal{P}_{\ell, \ell+n}^{\text{KK}} + \mathcal{P}_{\ell, \ell+n}^{\text{DK}} = \mathcal{P}_{\ell-1, \ell+n-1}^{\text{KK}} + \mathcal{P}_{\ell-1, \ell+n-1}^{\text{KD}} \quad (41)$$

$$\begin{aligned} &= \mathcal{P}_{\ell+1}^{(n-1)s} + \mathcal{P}_{\ell, \ell+n}^{\text{DK}} = \mathcal{P}_\ell^{(n-1)s} + \mathcal{P}_{\ell-1, \ell+n-1}^{\text{KD}} \\ &= \begin{array}{c} \text{\tiny $\ell$} \quad \text{\tiny $\ell+1$} \quad \dots \quad \text{\tiny $\ell+n$} \end{array} + \begin{array}{c} \text{\tiny $\ell$} \quad \text{\tiny $\ell+1$} \quad \dots \quad \text{\tiny $\ell+n$} \end{array} \\ &= \begin{array}{c} \text{\tiny $\ell-1$} \quad \text{\tiny $\ell$} \quad \dots \quad \text{\tiny $\ell+n-1$} \end{array} + \begin{array}{c} \text{\tiny $\ell-1$} \quad \text{\tiny $\ell$} \quad \dots \quad \text{\tiny $\ell+n-1$} \end{array}. \end{aligned}$$

The existence of two different decompositions of  $\mathcal{P}_\ell^{ns}$ , mimicking Eq. (22a), reflects the gauge freedom of MPSs. This can be exploited to write  $\mathcal{P}_{\ell, \ell+n}^{\text{DK}}$  as  $\mathcal{P}_\ell^{(n-1)s} + \mathcal{P}_{\ell-1, \ell-1+n}^{\text{KD}} - \mathcal{P}_{\ell+1}^{(n-1)s}$ , converting DK to KD, or vice versa. Repeated use yields an identity that will be useful below:

$$\sum_{\ell=\bar{\ell}}^{\ell'} \mathcal{P}_{\ell, \ell+n}^{\text{DK}} = \mathcal{P}_{\bar{\ell}}^{(n-1)s} + \sum_{\ell=\bar{\ell}}^{\ell'} \mathcal{P}_{\ell-1, \ell-1+n}^{\text{KD}} - \mathcal{P}_{\ell'+1}^{(n-1)s}. \quad (42)$$

### C. Global $ns$ projectors, $\mathbb{V}^{ns}$

We now are ready to define the  $ns$  spaces  $\mathbb{V}^{ns}$ . For  $n=0$ , we define  $\mathbb{V}^{0s} = \text{span}\{|\Psi\rangle\}$ . For  $n \geq 1$ , we define  $\mathbb{V}^{ns}$  as the span of  $|\Psi\rangle$  and all states  $|\Psi'\rangle$  differing from it on at most  $n$  contiguous sites:

$$\mathbb{V}^{ns} = \text{span}\left\{ \begin{array}{c} \text{\tiny $n$ sites} \\ \text{\tiny $\ell$} \quad \text{\tiny $\ell+1$} \quad \dots \quad \text{\tiny $\ell+n$} \end{array} \mid \ell \in [1, \mathcal{L}+1-n] \right\}. \quad (43)$$

For  $n=1$ ,  $\mathbb{V}^{1s}$  is the tangent space of  $|\Psi\rangle$ . More concretely,  $\mathbb{V}^{ns}$  is defined as the image of all local  $ns$  projectors:

$$\mathbb{V}^{ns} = \text{span}\left\{ \text{im}(\mathcal{P}_1^{ns}), \text{im}(\mathcal{P}_2^{ns}), \dots, \text{im}(\mathcal{P}_{\mathcal{L}+1-n}^{ns}) \right\}. \quad (44)$$

For any  $n' \leq n$ , the image  $\text{im}(\mathcal{P}_\ell^{n's})$  is by construction fully contained in the image  $\text{im}(\mathcal{P}_\ell^{ns})$ , hence  $\mathbb{V}^{n's}$  is a subspace of  $\mathbb{V}^{ns}$ , implying the nested hierarchy (1).

Let  $\mathcal{P}^{ns}$  be the projector having  $\mathbb{V}^{ns}$  as image; then,  $\text{im}(\mathcal{P}^{ns})$  contains  $\text{im}(\mathcal{P}_\ell^{ns})$  for all  $\ell \in [1, \mathcal{L}+1-n]$ . Formally,  $\mathcal{P}^{ns}$  has the defining properties

$$(\mathcal{P}^{ns})^2 = \mathcal{P}^{ns}, \quad \mathcal{P}^{ns} \mathcal{P}_\ell^{ns} = \mathcal{P}_\ell^{ns}, \quad (45a)$$

$$\mathcal{P}_\ell^{ns} |\Phi\rangle = 0 \quad \forall \ell \implies \mathcal{P}^{ns} |\Phi\rangle = 0. \quad (45b)$$

Moreover, the nested structure of the  $\mathbb{V}^{ns}$ s implies

$$\forall n' < n: \quad \mathcal{P}^{ns} \mathcal{P}^{n's} = \mathcal{P}^{n's}. \quad (46)$$

Let us construct  $\mathcal{P}^{ns}$  explicitly. Simply summing up the local projectors  $\mathcal{P}_\ell^{ns}$  does not yield a projector because the images of  $\mathcal{P}_\ell^{ns}$  and  $\mathcal{P}_{\ell'}^{ns}$  are not orthogonal. A set of mutually orthogonal local projectors can be obtained by projecting out the overlap between  $\mathcal{P}_\ell^{ns}$  and  $\mathcal{P}_{\ell\pm 1}^{ns}$ . We thus define

$$\mathcal{P}_{\ell\lesseqgtr}^{ns} = \mathcal{P}_\ell^{ns} (\mathbb{1}_V - \mathcal{P}_{\ell\pm 1}^{ns}), \quad (47)$$

so that  $\mathcal{P}_{\ell \leq}^{ns} \mathcal{P}_{\ell'}^{ns} = 0$  holds for neighboring  $\ell, \ell'$  with  $\ell \leq \ell'$ . It suffices to orthogonalize  $ns$  projectors mismatched by *one* site, since from these we can select a set of projectors mutually orthogonal on all sites. Indeed, Eqs. (39) and (41) yield  $(n-1)$ -site projectors containing DS,

$$\mathcal{P}_{\ell <}^{ns} = \mathcal{P}_{\ell}^{ns} - \mathcal{P}_{\ell+1}^{(n-1)s} = \mathcal{P}_{\ell, \ell+n}^{\text{DK}}, \quad (48a)$$

$$\mathcal{P}_{\ell >}^{ns} = \mathcal{P}_{\ell}^{ns} - \mathcal{P}_{\ell}^{(n-1)s} = \mathcal{P}_{\ell-1, \ell-1+n}^{\text{KD}}, \quad (48b)$$

and the DS ensure the orthonormality relations (cf. (34))

$$\mathcal{P}_{\ell \leq}^{ns} \mathcal{P}_{\ell' \leq}^{ns} = \delta_{\ell \ell'} \mathcal{P}_{\ell \leq}^{ns}, \quad (49a)$$

$$\forall \ell < \ell': \quad \mathcal{P}_{\ell <}^{ns} \mathcal{P}_{\ell' >}^{ns} = 0, \quad (49b)$$

$$\forall \ell \leq \ell': \quad \mathcal{P}_{\ell \leq}^{ns} \mathcal{P}_{\ell'}^{ns} = 0. \quad (49c)$$

These equations have a remarkable implication: for any choice of  $\ell' \in [1, \mathcal{L}-n+1]$ , the projectors  $\mathcal{P}_{\ell <}^{ns}$  for  $\ell \in [1, \ell'-1]$ ,  $\mathcal{P}_{\ell'}^{ns}$ , and  $\mathcal{P}_{\ell >}^{ns}$  for  $\ell \in [\ell'+1, \mathcal{L}+1-n]$  form an orthonormal set, and this set contains a  $\mathcal{P}_{\ell}^{ns}$  (in projected form) for *every*  $\ell \in [1, \mathcal{L}+1-n]$ . We define the global  $ns$  projector as their sum,

$$\begin{aligned} \mathcal{P}^{ns} &= \sum_{\ell=1}^{\ell'-1} \mathcal{P}_{\ell <}^{ns} + \mathcal{P}_{\ell'}^{ns} + \sum_{\ell=\ell'+1}^{\mathcal{L}+1-n} \mathcal{P}_{\ell >}^{ns} \\ &= \sum_{\ell=1}^{\ell'-1} \left( \text{Diagram: } \leftarrow \text{---} \text{---} \text{---} \rightarrow \right)_{\ell} + \left( \text{Diagram: } \leftarrow \text{---} \text{---} \text{---} \rightarrow \right)_{\ell'} + \sum_{\ell=\ell'+1}^{\mathcal{L}+1-n} \left( \text{Diagram: } \leftarrow \text{---} \text{---} \text{---} \rightarrow \right)_{\ell} \\ &\quad + \sum_{\ell=\ell'+1}^{\mathcal{L}+1-n} \left( \text{Diagram: } \leftarrow \text{---} \text{---} \text{---} \rightarrow \right)_{\ell-1} + \left( \text{Diagram: } \leftarrow \text{---} \text{---} \text{---} \rightarrow \right)_{\ell+n-1}. \end{aligned} \quad (50)$$

Here,  $\ell'$  may be chosen freely as convenience dictates; different choices are equivalent, being related by Eqs. (41). The orthogonality relations (49) ensure the properties (45a). For example,

$$\mathcal{P}^{ns} \mathcal{P}_{\ell'}^{ns} = 0 + \mathcal{P}_{\ell'}^{ns} \mathcal{P}_{\ell'}^{ns} + 0 = \mathcal{P}_{\ell'}^{ns}. \quad (51)$$

The property (45b) is ensured by orthogonalizing  $\mathcal{P}_{\ell}^{ns}$  w.r.t. each other and thus never including states with  $\mathcal{P}_{\ell}^{ns} |\Phi\rangle = 0 \forall \ell$ . This confirms that  $\text{im}(\mathcal{P}^{ns})$  contains  $\text{im}(\mathcal{P}_{\ell}^{ns})$  for all  $\ell \in [1, \mathcal{L}+1-n]$ ; thus,  $\mathcal{P}^{ns}$  indeed is the desired projector having  $\mathbb{V}^{ns}$  as image. Evaluating Eq. (50) using the middle expressions from (48), we obtain

$$\begin{aligned} \mathcal{P}^{ns} &= \sum_{\ell=1}^{\mathcal{L}+1-n} \mathcal{P}_{\ell}^{ns} - \sum_{\ell=1}^{\mathcal{L}-n} \mathcal{P}_{\ell+1}^{(n-1)s} \\ &= \sum_{\ell=1}^{\mathcal{L}+1-n} \left( \text{Diagram: } \leftarrow \text{---} \text{---} \text{---} \rightarrow \right)_{\ell} - \sum_{\ell=1}^{\mathcal{L}-n} \left( \text{Diagram: } \leftarrow \text{---} \text{---} \text{---} \rightarrow \right)_{\ell+1}, \end{aligned} \quad (52a)$$

expressing  $\mathcal{P}^{ns}$  through local  $ns$  and  $(n-1)s$  projectors in a manner manifestly independent of  $\ell'$ , and not involving any D sectors. The occurrence of the first term, a sum over all  $\mathcal{P}_{\ell}^{ns}$ , is no surprise; the nontrivial part of the above construction was establishing the form of the second term,

needed to ensure that  $\mathcal{P}^{ns}$  is a projector. Note that Eq. (52a) directly implies property (45b). Alternatively, we can use the rightmost forms of (48) in (50) to obtain

$$\mathcal{P}^{ns} = \sum_{\ell=1}^{\ell'} \mathcal{P}_{\ell, \ell+n}^{\text{DK}} + \mathcal{P}_{\ell', \ell'+n}^{\text{KK}} + \sum_{\ell=\ell'}^{\mathcal{L}-n} \mathcal{P}_{\ell, \ell+n}^{\text{KD}}, \quad (52b)$$

now expressed purely through  $(n-1)s$  projectors, with all but one involving D sectors.

For  $n=1$ , Eqs. (52) reproduce the well-known tangent space projector,

$$\mathcal{P}^{1s} = \sum_{\ell=1}^{\mathcal{L}} \mathcal{P}_{\ell}^{1s} - \sum_{\ell=1}^{\mathcal{L}-1} \mathcal{P}_{\ell}^b \quad (53a)$$

$$\begin{aligned} &= \sum_{\ell=1}^{\mathcal{L}} \left( \text{Diagram: } \leftarrow \text{---} \text{---} \text{---} \rightarrow \right)_{\ell} - \sum_{\ell=1}^{\mathcal{L}-1} \left( \text{Diagram: } \leftarrow \text{---} \text{---} \text{---} \rightarrow \right)_{\ell} \\ &= \sum_{\ell=1}^{\ell'} \mathcal{P}_{\ell, \ell+1}^{\text{DK}} + \mathcal{P}_{\ell', \ell'+1}^{\text{KK}} + \sum_{\ell=\ell'}^{\mathcal{L}-1} \mathcal{P}_{\ell, \ell+1}^{\text{KD}} \\ &= \sum_{\ell=1}^{\ell'} \left( \text{Diagram: } \leftarrow \text{---} \text{---} \text{---} \rightarrow \right)_{\ell} + \left( \text{Diagram: } \leftarrow \text{---} \text{---} \text{---} \rightarrow \right)_{\ell'} + \sum_{\ell=\ell'}^{\mathcal{L}-1} \left( \text{Diagram: } \leftarrow \text{---} \text{---} \text{---} \rightarrow \right)_{\ell}. \end{aligned} \quad (53b)$$

These expressions are widely used in MPS algorithms based on tangent space concepts, such as time evolution using the time-dependent variational principle (TDVP) [11–14, 30]. The form (53a), or (53b) with the choice  $\ell' = \mathcal{L}-1$ , was first given Lubich, Oseledts and Vandereycken [11] (Theorem 3.1), and transcribed into MPS notation in Ref. [12]. In these works, it was derived in a different manner than here, using arguments invoking gauge invariance. Our derivation has the advantage that it generalizes directly to  $ns$  projectors. For  $n=2$ , our expression (52a) for  $\mathcal{P}^{2s}$  reproduces the projector proposed in Ref. [12] for 2s TDVP:

$$\mathcal{P}^{2s} = \sum_{\ell=1}^{\mathcal{L}-1} \left( \text{Diagram: } \leftarrow \text{---} \text{---} \text{---} \rightarrow \right)_{\ell} - \sum_{\ell=2}^{\mathcal{L}-1} \left( \text{Diagram: } \leftarrow \text{---} \text{---} \text{---} \rightarrow \right)_{\ell}. \quad (54)$$

#### D. Irreducible global $ns$ projectors, $\mathcal{P}^{n\perp}$

Our final step is to orthogonalize the global  $\mathcal{P}^{ns}$  projectors to obtain mutually *orthogonal* global  $ns$  projectors,  $\mathcal{P}^{n\perp}$ . This step is inspired by the observation, made in Ref. 6, that a given MPS  $|\Psi\rangle$  induces a decomposition of the full Hilbert space into mutually orthogonal subspaces,

$$\mathbb{V} = \oplus_{n=0}^{\mathcal{L}} \mathbb{V}^{n\perp}, \quad (55)$$

where  $\mathbb{V}^{0\perp}$  is spanned by  $|\Psi\rangle$ , and for  $n \geq 1$  each  $\mathbb{V}^{n\perp}$  is the complement of  $\mathbb{V}^{(n-1)s}$  in  $\mathbb{V}^{ns} = \mathbb{V}^{(n-1)s} \oplus \mathbb{V}^{n\perp}$ .







$$\Delta_E^{(n \geq 2)\perp} = \sum_{\ell=1}^{\mathcal{L}-(n-1)} \left\| \text{Diagram} \right\|^2. \quad (68b)$$

The second equality in Eq. (68a) follows from Eq. (20). To compute these expressions in practice, the  $\mathbb{D}$  projectors are expressed through  $\mathbb{K}$  projectors using Eq. (21), e.g.

$$\Delta_E^{1\perp} = \sum_{\ell=1}^{\mathcal{L}} \left\| \text{Diagram} - \text{Diagram} \right\|^2. \quad (69)$$

If the Hamiltonian contains only local and nearest-neighbor terms, all contributions with  $n > 2$  are zero [6], i.e.  $\Delta_E = \Delta_E^{2s}$ . However, it has been argued in Ref. 6 that even if long-range terms are present,  $\Delta_E^{2s}$  is a reliable error measure. Here, we confirm this for the case of the spin- $\frac{1}{2}$  Haldane-Shastry model on a ring of length  $\mathcal{L} = 40$ , with Hamiltonian

$$\mathcal{H}_{\text{HS}} = \sum_{\ell < \ell' \leq \mathcal{L}} \frac{\pi^2 \mathbf{S}_\ell \cdot \mathbf{S}_{\ell'}}{\mathcal{L}^2 \sin^2 \frac{\pi}{\mathcal{L}} (\ell - \ell')}. \quad (70)$$

Figure 1 shows  $\Delta_E^{n\perp}$  for  $n \in \{1, 2, \dots, 10\}$  and four choices of  $D^*$ . In all cases,  $\Delta_E^{n\perp}$  is largest for  $n = 2$ , and smaller by an order magnitude or more for  $n > 2$ , with the decrease being stronger the larger  $D^*$ . For this model, therefore,  $\Delta_E^{2\perp}$  by itself suffices to reliably estimate the energy error.

## V. $n$ -SITE EXCITATIONS

The  $ns$  projectors can be used as an Ansatz to compute low energy excitations. This so-called excitation Ansatz has been very successful in infinite systems [14, 22, 28, 32, 33] and lately also shown to be reliable on finite lattices [34]. Using our diagrammatic

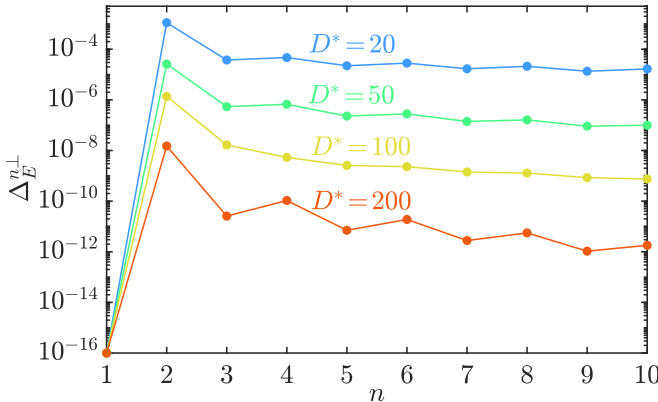


FIG. 1. The  $n$ -site variance,  $\Delta_E^{n\perp}$ , of the  $\mathcal{L} = 40$  Haldane-Shastry model for different  $D^*$ .  $\Delta_E^{1\perp}$  can in principle always be converged to numerically zero (i.e.  $\Delta_E^{1\perp} \lesssim 10^{-16}$ ) by extensive DMRG sweeping; this being the case here, we plot it symbolically at  $\Delta_E^{1\perp} = 10^{-16}$ . In practice it suffices to sweep until  $\Delta_E^{1\perp} \ll \Delta_E^{2\perp}$ , since the variance is dominated by  $\Delta_E^{2\perp}$ .

notation, we generalize the 1s Ansatz for finite systems used in Ref. 34 to  $n$  sites, similar to the  $ns$  Ansatz for infinite systems [22, 28].

We seek an  $ns$  excitation Ansatz satisfying the condition  $\mathcal{P}^{ns} |\Psi_{\text{ex}}^{ns}\rangle = |\Psi_{\text{ex}}^{ns}\rangle$ . Let us choose  $\ell' = \mathcal{L} - n + 1$  in Eq. (50), such that  $\mathcal{P}^{ns} = \sum_{\ell=1}^{\mathcal{L}-n} \mathcal{P}_{\ell}^{ns} + \mathcal{P}_{\ell'}^{ns}$ . Then, the following Ansatz has the desired property:

$$\begin{aligned} |\Psi_{\text{ex}}^{ns}\rangle &= \sum_{\ell=1}^{\mathcal{L}-n} \text{Diagram} + \text{Diagram} \\ &= \sum_{\ell=1}^{\mathcal{L}-n+1} \text{Diagram}. \end{aligned} \quad (71)$$

Here,  $T_{i>1}^\ell$  ( $\odot$ ) are generic tensors of rank 3 and

$$T_1^\ell = \odot = \begin{cases} \text{Diagram} & \ell < \ell', \\ \text{Diagram} & \ell = \ell', \end{cases} \quad \ell' = \mathcal{L} - n + 1. \quad (72)$$

The two forms of  $T_1^\ell$  reflect the presence or absence of a  $\mathbb{D}$  projection associated with  $\mathcal{P}_{\ell}^{ns}$  or  $\mathcal{P}_{\ell'}^{ns}$ , respectively.

It seems that  $|\Psi_{\text{ex}}^{ns}\rangle$  cannot be efficiently computed, since it involves a sum over  $\mathcal{L} - n + 1$  (i.e. many!) terms, and performing MPS sums explicitly leads to increased bond dimensions. However, that can be avoided here. The isometries  $A_\ell$  ( $\nabla$ ) and  $B_\ell$  ( $\nabla$ ) flanking the modified sites reappear in every summand and only need to be saved once; hence only the tensors  $T_i^\ell$  need to be saved. In the case of  $n = 1$  for example, we have to save  $\mathcal{L}$  tensors of dimensions  $D \times d \times D$ , i.e. the same memory requirement as for an MPS with bond dimension  $D$ .

Moreover, Eq. (72) ensures that all summands are by construction mutually orthogonal, facilitating the computation of overlaps. Consider  $|\Psi_{\text{ex}}^{ns}\rangle$  and  $|\Psi_{\text{ex}}'^{ns}\rangle$ , characterized by  $T_i^\ell$  and  $T_i'^\ell$ , respectively. Due to Eq. (72), their overlap involves only  $\mathcal{L} - n + 1$  terms (not that number squared), namely

$$\langle \Psi_{\text{ex}}'^{ns} | \Psi_{\text{ex}}^{ns} \rangle = \sum_{\ell=1}^{\mathcal{L}-n+1} \text{Diagram}, \quad (73)$$

while the computation of sums or differences can be done on the level of the  $T_i^\ell$ , i.e.

$$|\Psi_{\text{ex}}^{ns}\rangle + a |\Psi_{\text{ex}}'^{ns}\rangle \rightarrow \forall \ell : \text{Diagram} + a \text{Diagram}. \quad (74)$$

If  $\prod_{i=1}^n T_i^\ell$  and  $\prod_{i=1}^n T_i'^\ell$  are represented as MPSs, Eq. (74) in effect involves a sum of two  $ns$  MPSs; this is manageable if  $n$  is not too large. In the case  $n = 1$ , there is only  $T_1^\ell$  and  $T_1'^\ell$ , i.e. in this case, no MPS sums are required.

A further benefit of Eq. (72) is that it serves to fix the MPS gauge degree of freedom on the site hosting  $T_1^\ell$ , improving numerical stability.

To determine the tensors  $T_i^\ell$  for  $|\Psi_{\text{ex}}^{ns}\rangle$  explicitly, one projects the Hamiltonian onto the space  $\mathbb{V}^{ns}$  and solves for low-energy states of

$$\mathcal{P}^{ns} H \mathcal{P}^{ns} |\Psi_{\text{ex}}^{ns}\rangle = E_{\text{ex}}^{ns} |\Psi_{\text{ex}}^{ns}\rangle \quad (75)$$

that are orthogonal to the ground state. This can be done using some iterative eigensolver like the Lanczos method, initialized by some appropriate initial wavefunction. Explicit orthogonalization w.r.t. to the ground state is required, since our Ansatz space  $\mathcal{P}^{ns}$  contains the ground state, whose kept and discarded spaces span the image of  $\mathcal{P}^{ns}$ .

To run an iterative eigensolver, a scheme is needed for efficiently applying the projected Hamiltonian  $\mathcal{P}^{ns} H \mathcal{P}^{ns}$  to the state  $|\Psi_{\text{ex}}^{ns}\rangle$ . The resulting state, say  $|\bar{\Psi}_{\text{ex}}^{ns}\rangle = \mathcal{P}^{ns} H \mathcal{P}^{ns} |\Psi_{\text{ex}}^{ns}\rangle$ , will again be of the form (71), but described by tensors  $\bar{T}_i^\ell$ . To find these, we compute the tensors

$$\tilde{T}_1^\ell \bar{T}_2^\ell \bar{T}_n^\ell = \sum_{\ell'=1}^{\mathcal{L}-n+1} \left( \text{MPS diagram with } T_1^{\ell'}, \dots, T_n^{\ell'} \right), \quad (76)$$

and project  $\tilde{T}_1^\ell$  to the discarded space to obtain  $\bar{T}_1^\ell$ ,

$$\bar{T}_1^\ell = \tilde{T}_1^\ell - (1 - \delta_{\ell, \mathcal{L}-n+1}) \left( \text{MPS diagram with } T_1^{\ell'} \right), \quad (77)$$

such that Eq. (72) is fulfilled.

To evaluate Eq. (76), we split the sum  $\sum_{\ell'}$  into terms with  $\ell' < \ell$  and  $\ell' \geq \ell$ , and express these as follows:

$$\begin{aligned} \tilde{T}_1^\ell \bar{T}_2^\ell \bar{T}_n^\ell &= \sum_{m=1}^n \left( \text{MPS diagram with } T_{\ell-1}^{\ell-m}, T_\ell^{\ell-m}, T_{\ell+1}^{\ell-m} \right) R_{\ell+n}^m \\ &\quad + \sum_{m=0}^n \left( \text{MPS diagram with } T_{\ell-1}^{\ell+m}, T_\ell^{\ell+m}, T_{\ell+1}^{\ell+m} \right) R_{\ell+n}^m. \end{aligned} \quad (78)$$

Next to the left and right environments  $L_\ell$  and  $R_\ell$  defined in Eq. (18), these expressions contain another set of environments, denoted by  $\mathcal{L}_\ell^m$  and  $\mathcal{R}_\ell^m$ , each involving those  $m$  of the  $T_i^{\ell'}$  tensors in Eq. (76) that do not face open physical legs. For  $m = 0$ ,  $m \in \{1, \dots, n-1\}$  or  $m = n$ , they are defined by the left equalities below; the right equalities show how for each  $m$ ,  $\mathcal{L}_{\ell+1}^m$  and  $\mathcal{R}_{\ell-1}^m$  can be computed recursively from  $\mathcal{L}_\ell^m$  and  $\mathcal{R}_\ell^m$ , initialized with  $\mathcal{L}_0^0 = 1$ ,  $\mathcal{L}_0^{m>0} = 0$ ,  $\mathcal{R}_{\mathcal{L}+1}^0 = 1$ ,  $\mathcal{R}_{\mathcal{L}+1}^{m>0} = 0$ :

$$\mathcal{L}_\ell^0 = \left[ \begin{array}{c} \text{MPS diagram} \end{array} \right] = \left[ \begin{array}{c} \text{MPS diagram} \end{array} \right] = \left[ \begin{array}{c} \text{MPS diagram} \end{array} \right], \quad (79a)$$

$$\mathcal{L}_\ell^m = \left[ \begin{array}{c} \text{MPS diagram} \end{array} \right] = \left[ \begin{array}{c} \text{MPS diagram} \end{array} \right] = \left[ \begin{array}{c} \text{MPS diagram} \end{array} \right],$$

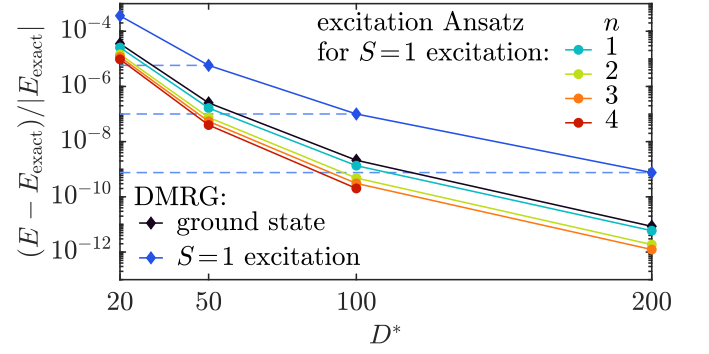


FIG. 2. Relative error in energy of the lowest-lying  $S = 1$  excited state of the Haldane-Shastry model, computed using the  $n$ -site excitation Ansatz (circles), or using DMRG (blue diamonds). Black diamonds show DMRG results for the  $S = 0$  ground state. The dashed blue lines are guides to the eye.

$$\begin{aligned} \mathcal{L}_\ell^n &= \left[ \begin{array}{c} \text{MPS diagram} \end{array} \right] = \sum_{\ell'=1}^{\ell-n+1} \left[ \begin{array}{c} \text{MPS diagram} \end{array} \right] = \left[ \begin{array}{c} \text{MPS diagram} \end{array} \right] + \left[ \begin{array}{c} \text{MPS diagram} \end{array} \right], \\ \mathcal{R}_\ell^0 &= \left[ \begin{array}{c} \text{MPS diagram} \end{array} \right] = \left[ \begin{array}{c} \text{MPS diagram} \end{array} \right], \end{aligned} \quad (79b)$$

$$\mathcal{R}_\ell^m = \left[ \begin{array}{c} \text{MPS diagram} \end{array} \right] = \left[ \begin{array}{c} \text{MPS diagram} \end{array} \right] = \left[ \begin{array}{c} \text{MPS diagram} \end{array} \right],$$

$$\mathcal{R}_\ell^n = \left[ \begin{array}{c} \text{MPS diagram} \end{array} \right] = \sum_{\ell'=\ell}^{\mathcal{L}-n+1} \left[ \begin{array}{c} \text{MPS diagram} \end{array} \right] = \left[ \begin{array}{c} \text{MPS diagram} \end{array} \right] + \left[ \begin{array}{c} \text{MPS diagram} \end{array} \right].$$

The solution of Eq. (75) using an iterative eigensolver has costs scaling with  $\mathcal{O}(D^3 d^n w)$ , the same as  $ns$  DMRG. However, because the Ansatz Eq. (71) is built from a sum over  $\mathcal{L} - n + 1$  MPSSs, states can be captured which would need significantly larger bond dimensions if represented in standard fashion as an MPS. Because there are  $n$  summands in Eq. (71) which differ from the ground state at site  $\ell$  (with corresponding tensors  $T_1^\ell, \dots, T_n^{\ell-n+1}$  at site  $\ell$ ), an MPS representation would need bond dimension  $D(1+n)$ , assuming  $A_\ell$ ,  $B_\ell$  and  $T_i^\ell$  are tensors of dimension  $D \times d \times D$ . Optimizing such an MPS with  $ns$  DMRG comes with  $\mathcal{O}(D^3(n+1)^3 d^n w)$  costs, larger by  $(n+1)^3$  than the costs for optimizing the Ansatz Eq. (71). Of course, the latter Ansatz is much more restrictive than a generic MPS of bond dimension  $D(1+n)$ . However, that should not be a limitation if the physics of interest involves single- or few-particle excitations, as is the case, e.g., when computing correlations functions of single- or few-particle operators.

We test the  $ns$  excitation Ansatz on a Haldane-Shastry model on a ring of length  $\mathcal{L} = 40$  (see Eq. (70) for the Hamiltonian), for which we seek to compute the lowest energy excitation with total spin  $S = 1$  above the total spin  $S = 0$  ground state. For comparison, we have also computed this state by performing a DMRG ground state



search in the  $S = 1$  sector.

Fig. 2 shows the corresponding relative errors in energy versus the bond dimension  $D^*$ . As reference values, we use the exact energies  $E_{\text{exact}}^{S=0} = -\pi^2(\mathcal{L} + 5/\mathcal{L})/24$  and  $E_{\text{exact}}^{S=1} = -\pi^2(\mathcal{L} - 7/\mathcal{L})/24$  for the ground state and excited state [35–37], respectively. Remarkably, we find that for the same  $D^*$ , the  $n=1$  site excitation Ansatz yields an  $S = 1$  excitation energy that is more accurate than that obtained from DMRG by one to two orders of magnitude, even though the computational cost of both approaches at the same  $D^*$  is comparable. In fact, the relative error obtained by the excitation Ansatz for the  $S = 1$  state is comparable to (even slightly lower than) that obtained by DMRG for the  $S = 0$  ground state.

The reason for the high accuracy of the excitation Ansatz is that the first excited state of the Haldane-Shastry model is essentially a superposition of local spin excitations, i.e. it fits Ansatz (71). The excitation Ansatz avoids representing this superposition as a single MPS, which would require about twice the bond dimension. Instead, it exploits the fact that each local excitation differs from the ground state only locally. This leads to a more economic Ansatz compared to DMRG, which needs about twice the bond dimension. This can also be seen in Fig. 2, where the relative error in energy of the 1s excitation Ansatz at some  $D^*$  almost coincides with the corresponding error of DMRG at  $2D^*$ . The latter error is slightly smaller than the former, because the  $2D^*$  MPS Ansatz used by DMRG is less restrictive than the  $D^*$  excitation Ansatz, though this improvement is rather marginal.

The capability of the excitation Ansatz can be further improved by considering  $n > 1$ , leading to a reduction of the relative error in energy compared to  $n=1$ , see Fig. 2. This reduction is rather small and further improvements seem to become ever smaller for ever larger  $n$ . However, with increasing  $n$  the costs for this Ansatz increase exponentially, as  $\sim d^n$ . Therefore, including information beyond  $n=1$  by brute force, i.e. by just going to  $n > 1$ , is not advisable. Nevertheless, we believe that valuable improvements of the Ansatz may be achievable, while circumventing the exponential  $d^n$  scaling, by including only those parts of the  $n > 1$  sectors that contribute to the excited state with significant weight. It should be possible to identify these parts by generalizing the strategy proposed in our recent work on controlled bond expansion in both DMRG ground state search [29] and TDVP time evolution [30]. We leave this as a topic for future study.

More generally, we believe that the diagrammatics for the  $n$ -site excitation Ansatz and the projector formalism developed in this work will provide a solid foundation to construct systematic improvements to the 1-site excitation Ansatz without a significant increase in computational costs.

We conclude this section by noting that the above construction will not be able to find states that differ from a given ground state on an extensive number of sites. In particular, if the ground state sector has a degeneracy,

e.g. due to symmetry breaking or topological order, the excitation Ansatz on top of one of the ground states is not expected to reliably find the other ground states.

Further, while the excitation Ansatz Eq. (71) can in principle be used for excitations at any energy, it is expected to perform less reliable the higher the energy of the excitation. Examples, where the Ansatz Eq. (71) should have problems, are excitations of multiple independent particles (i.e. the particles may be located far apart from each other) or excited states with a volume-law entanglement entropy.

## VI. SUMMARY AND OUTLOOK

We have developed a projector formalism for kept and discarded spaces of MPS, together with a convenient diagrammatic notation. We use it to derive explicit expressions for global  $n$ -site projectors  $\mathcal{P}^{ns}$  and irreducible  $n$ -site projectors  $\mathcal{P}^{n\perp}$ . We then use our results to derive explicit formulas for the  $n$ -site variance and evaluate it for the Haldane-Shastry model, showing that indeed the 2-site contribution is the most dominant one. Further, we derive explicit diagrammatic formulas to perform excited state computations based on the  $n$ -site excitation Ansatz for finite, non-translation invariant MPS.

The  $\kappa, \mathcal{D}$  projector formalism and diagrammatic notation developed here proved very convenient for the applications considered in this work. More generally, we expect them to provide a convenient tool for the development of new MPS algorithms that explicitly or implicitly utilize the properties of discarded spaces. The information contained in these is a *resource*, useful for describing changes or variations of a given MPS, and for algorithms exploiting this resource, the  $\kappa, \mathcal{D}$  projector formalism facilitates book-keeping thereof. Indeed, we have developed the formalism presented here while working out a controlled bond expansion algorithm to perform both DMRG ground-state searches [29] and time evolutions using the time-dependent variational principle [30] with 2-site accuracy at 1-site computational cost. Moreover, our formalism provides the tools needed to efficiently implement the perspectives outlined in Refs. 14 and 22 for post-MPS applications, that build on a given MPS to compute low energy excitation spectra.

As a final remark, we note that though we focused on MPSs in this work, our formalism should be generalizable to any tensor network for which canonical forms are available, such as tensor networks without loops.

## ACKNOWLEDGEMENTS

We thank Andreas Weichselbaum for stimulating discussions, and Seung-Sup Lee, Juan Espinoza, Matan Lotem, Jeongmin Shim and Andreas Weichselbaum for helpful comments on the manuscript. Our numerical simulations employed the QSpace tensor library [38, 39]. This research



was funded in part by the Deutsche Forschungsgemeinschaft under Germany's Excellence Strategy EXC-2111

(Project No. 390814868), and is part of the Munich Quantum Valley, supported by the Bavarian state government with funds from the Hightech Agenda Bayern Plus.

- 
- [1] S. R. White, Density matrix formulation for quantum renormalization groups, *Phys. Rev. Lett.* **69**, 2863 (1992).
  - [2] S. R. White, Density-matrix algorithms for quantum renormalization groups, *Phys. Rev. B* **48**, 10345 (1993).
  - [3] A. J. Daley, C. Kollath, U. Schollwöck, and G. Vidal, Time-dependent density-matrix renormalization-group using adaptive effective Hilbert spaces, *J. Stat. Mech.: Theor. Exp.* **P04005** (2004).
  - [4] S. R. White, Density matrix renormalization group algorithms with a single center site, *Phys. Rev. B* **72**, 180403 (2005).
  - [5] C. Hubig, I. P. McCulloch, U. Schollwöck, and F. A. Wolf, Strictly single-site DMRG algorithm with subspace expansion, *Phys. Rev. B* **91**, 155115 (2015).
  - [6] C. Hubig, J. Haegeman, and U. Schollwöck, Error estimates for extrapolations with matrix-product states, *Phys. Rev. B* **97**, 045125 (2018).
  - [7] G. Vidal, Efficient classical simulation of slightly entangled quantum computations, *Phys. Rev. Lett.* **91**, 147902 (2003).
  - [8] G. Vidal, Efficient simulation of one-dimensional quantum many-body systems, *Phys. Rev. Lett.* **93**, 040502 (2004).
  - [9] G. Vidal, Classical simulation of infinite-size quantum lattice systems in one spatial dimension, *Phys. Rev. Lett.* **98**, 070201 (2007).
  - [10] J. Haegeman, J. I. Cirac, T. J. Osborne, I. Pižorn, H. Verschelde, and F. Verstraete, Time-dependent variational principle for quantum lattices, *Phys. Rev. Lett.* **107**, 070601 (2011).
  - [11] C. Lubich, I. V. Oseledets, and B. Vandereycken, Time integration of tensor trains, *SIAM J. Numer. Anal.* **53**, 917 (2015).
  - [12] J. Haegeman, C. Lubich, I. Oseledets, B. Vandereycken, and F. Verstraete, Unifying time evolution and optimization with matrix product states, *Phys. Rev. B* **94**, 165116 (2016).
  - [13] V. Zauner-Stauber, L. Vanderstraeten, M. T. Fishman, F. Verstraete, and J. Haegeman, Variational optimization algorithms for uniform matrix product states, *Phys. Rev. B* **97**, 045145 (2018).
  - [14] L. Vanderstraeten, J. Haegeman, and F. Verstraete, Tangent-space methods for uniform matrix product states, *SciPost Phys. Lect. Notes* **7** (2019).
  - [15] K. G. Wilson, The renormalization group: Critical phenomena and the Kondo problem, *Rev. Mod. Phys.* **47**, 773 (1975).
  - [16] R. Peters, T. Pruschke, and F. B. Anders, Numerical renormalization group approach to Green's functions for quantum impurity models, *Phys. Rev. B* **74**, 245114 (2006).
  - [17] A. Weichselbaum and J. von Delft, Sum-rule conserving spectral functions from the numerical renormalization group, *Phys. Rev. Lett.* **99**, 076402 (2007).
  - [18] K. A. Hallberg, Density-matrix algorithm for the calculation of dynamical properties of low-dimensional systems, *Phys. Rev. B* **52**, 9827(R) (1995).
  - [19] T. D. Kühner and S. R. White, Dynamical correlation functions using the density matrix renormalization group, *Phys. Rev. B* **60**, 335 (1999).
  - [20] E. Jeckelmann, Dynamical density-matrix renormalization-group method, *Phys. Rev. B* **66**, 045114 (2002).
  - [21] A. Holzner, A. Weichselbaum, I. P. McCulloch, U. Schollwöck, and J. von Delft, Chebyshev matrix product state approach for spectral functions, *Phys. Rev. B* **83**, 195115 (2011).
  - [22] J. Haegeman, T. J. Osborne, and F. Verstraete, Post-matrix product state methods: To tangent space and beyond, *Phys. Rev. B* **88**, 075133 (2013).
  - [23] U. Schollwöck, The density-matrix renormalization group in the age of matrix product states, *Annals of Physics* **326**, 96 (2011).
  - [24] A. Weichselbaum, Tensor networks and the numerical renormalization group, *Phys. Rev. B* **86**, 245124 (2012).
  - [25] S. Paeckel, T. Köhler, A. Swoboda, S. R. Manmana, U. Schollwöck, and C. Hubig, Time-evolution methods for matrix-product states, *Annals of Physics* **411**, 167998 (2019).
  - [26] F. B. Anders and A. Schiller, Real-time dynamics in quantum-impurity systems: A time-dependent numerical renormalization-group approach, *Phys. Rev. Lett.* **95**, 196801 (2005).
  - [27] S.-S. B. Lee, F. B. Kugler, and J. von Delft, Computing local multipoint correlators using the numerical renormalization group, *Phys. Rev. X* **11**, 041007 (2021).
  - [28] J. Haegeman, S. Michalakakis, B. Nachtergaele, T. J. Osborne, N. Schuch, and F. Verstraete, Elementary excitations in gapped quantum spin systems, *Phys. Rev. Lett.* **111**, 080401 (2013).
  - [29] A. Gleis, J.-W. Li, and J. von Delft, Controlled bond expansion for DMRG ground state search at single-site costs, *arXiv:2207.14712 [cond-mat.str-el]* (2022).
  - [30] J.-W. Li, A. Gleis, and J. von Delft, Time-dependent variational principle with controlled bond expansion for matrix product states, *arXiv:2208.10972 [cond-mat.str-el]* (2022).
  - [31] F. B. Kugler, S.-S. B. Lee, and J. von Delft, Multipoint correlation functions: Spectral representation and numerical evaluation, *Phys. Rev. X* **11**, 041006 (2021).
  - [32] J. Haegeman, B. Pirvu, D. J. Weir, J. I. Cirac, T. J. Osborne, H. Verschelde, and F. Verstraete, Variational matrix product ansatz for dispersion relations, *Phys. Rev. B* **85**, 100408 (2012).
  - [33] W.-L. Tu, H.-K. Wu, N. Schuch, N. Kawashima, and J.-Y. Chen, Generating function for tensor network diagrammatic summation, *Phys. Rev. B* **103**, 205155 (2021).
  - [34] M. Van Damme, R. Vanhove, J. Haegeman, F. Verstraete, and L. Vanderstraeten, Efficient matrix product state methods for extracting spectral information on rings and cylinders, *Phys. Rev. B* **104**, 115142 (2021).
  - [35] T. Yamamoto, Y. Saiga, M. Arikawa, and Y. Kuramoto, Exact dynamical structure factor of the degenerate

- Haldane-Shastry model, *Phys. Rev. Lett.* **84**, 1308 (2000).
- [36] T. Yamamoto, Y. Saiga, M. Arikawa, and Y. Kuramoto, Exact dynamics of the  $SU(K)$  Haldane-Shastry model, *Journal of the Physical Society of Japan* **69**, 900 (2000).
- [37] Y.-H. Wu, L. Wang, and H.-H. Tu, Tensor network representations of parton wave functions, *Phys. Rev. Lett.* **124**, 246401 (2020).
- [38] A. Weichselbaum, Non-abelian symmetries in tensor networks: A quantum symmetry space approach, *Ann. of Phys.* **327**, 2972 (2012).
- [39] A. Weichselbaum, X-symbols for non-abelian symmetries in tensor networks, *Phys. Rev. Research* **2**, 023385 (2020).